工學碩士 學位論文

해수의 간접탄산화를 이용한 고순도 배터라이트형 및 칼사이트형 탄산칼슘의 제조방법

Method for producing high purity vaterite and calcite calcium carbonate using indirect carbonation of seawater

指導敎授 김 명 진
共同指導敎授 박 영 규

2019 年 8 月

韓國海洋大學校 海洋科學技術專門大學院

海洋科學技術融合學科
전 준 혁

본 논문을 전준혁의 공학석사 학위논문으로 인준함

위원장 : 유 경 근 인
위 원 : 김 명 진 인
위 원 : 박 영 규 인

2019 년 07 월

한국해양대학교 해양과학기술전문대학원

Contents

List of Tables

List of Figures

해수의 간접탄산화를 이용한 고순도 배터라이트형 및 칼사이트형 탄산칼슘의 제조방법

전준혁

한국해양대학교 해양과학기술전문대학원
해양과학기술융합학과

초록

간접탄산화는 대표적인 이산화탄소 포집 저장 및 활용 기술이다. 간접탄산화 기술 중 화학 용제의 비용이 기술비용의 대부분을 차지하므로 기술의 경제성을 확보하기 어려웠다. 이를 극복하기 위해 본 연구에서는 간접탄산화에서 값비싼 화학용제 대신에 저비용 혹은 무상의 해수를 반응의 용제로 사용하였다. 본 연구에서는 알칼리 산업부산물인 시멘트 킬른 더스트(CKD)와 해수를 사용하였다. 해수를 사용하여도 기존의 간접탄산화 기술에 사용되어 왔던 용제들과 비교하여 많은양의 이산화탄소를 저장할 수 있었고, 고순도의 탄산칼슘을 생성할 수 있었다. CKD로부터 칼슘을 용출하는 해수의 성분은 마그네슘으로 나타났다. CKD와 해수의 고액비는 칼슘 용출 효율에 가장 큰 영향을 미치는 인자였으며, 이산화탄소 유량과 NaOH 첨가량은 탄산화 효율에 가장 큰 영향을 미쳤다. 생성된 탄산칼슘은 calcite와 vaterite 였으며, 최대 99.4%의 순도를 나타내었다. 이산화탄소 저장량과 탄산칼슘 생성량은 각

각 185kg-CO_2/ton-CKD, 419kg-$CaCO_3$/ton-CKD 로 나타났다. 해수에 마그네슘을 첨가한다면 이 값들은 최대 271kg-CO_2/ton-CKD, 615kg-$CaCO_3$/ton-CKD 로 크게 증가하였다. 간접탄산화 반응을 통해 생성되는 침강성 탄산칼슘의 한 종류인 vaterite형 탄산칼슘은 높은 용해도 등의 특성 때문에 다른 형태의 탄산칼슘 보다 더 다양한 용도에 사용이 가능하다. 기존 간접탄산화 반응의 용제들과 비교하여 해수는 vaterite형 탄산칼슘 생성에 매우 유리하였고, 생성되는 탄산칼슘의 입자크기 또한 작게 나타났다. 해수와 다양한 원료를 간접탄산화 반응에 사용하였을 때, 원료에 관계 없이 모두 높은 함량의 vaterite를 생성할 수 있었다. 하지만 해수를 이용한 탄산화반응 시 교반 임펠러의 크기, 교반속도의 조건이 만족되어야 100% vaterite형 탄산칼슘을 생성할 수 있었다.

주제어: Seawater 해수; Indirect carbonation 간접탄산화; Industrial by-products 산업부산물; Mg 마그네슘; Vaterite 배터라이트.

Chapter 1. Introduction

1.1 Introduction

The concentration of CO_2 in the atmosphere is steadily increasing. According to a report by the Intergovernmental Panel on Climate Change, it is predicted that the concentration of atmospheric CO_2 will increase to 1200 ppm by 2100 (IPCC, 2007). Shaffer (2010) predicted that the global average temperature will rise by 5 °C in 2030 and temperature of seawater also will rise by 3 °C in 4010, using simulations of predicted greenhouse gas emissions. In order to reduce CO_2 worldwide, research has mainly focused on carbon dioxide capture and storage to store CO_2 underground or in the ocean floor that called carbon dioxide capture and storage (CCS). However, research on carbon dioxide capture, utilization, and storage (CCUS) technology for recycling CO_2 is attracting new attention (Azdarpour et al., 2015; Sanna et al., 2014; Markewitz et al., 2012; Prigiobbe et al., 2009).

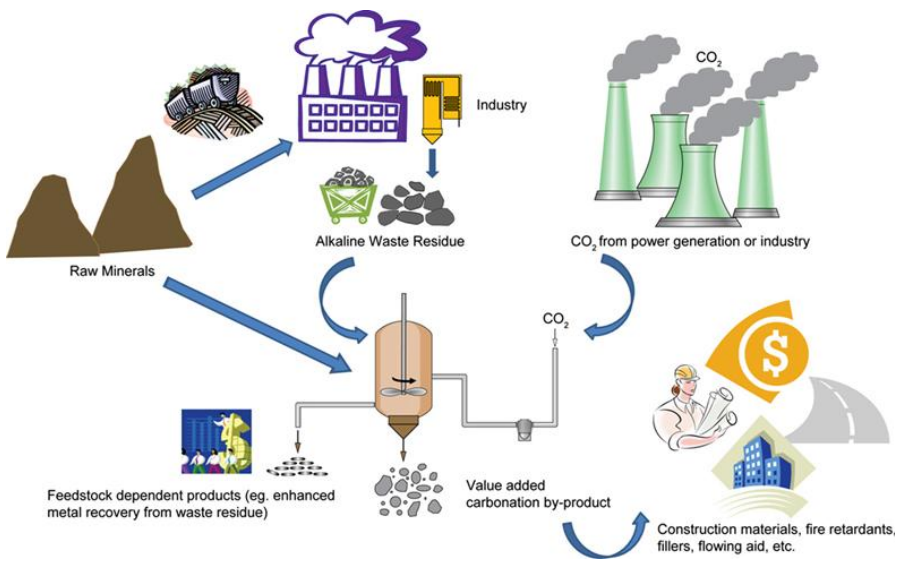

Fig. 1 Concept of mineral carbonation (Bobicki et al., 2012)

An example of CCS technology is mineral carbonation (Fig 1). It is a technique of storing CO_2 in the form of insoluble carbonate minerals that are thermodynamically stable by reacting with raw materials containing Ca or Mg (Bobicki et al., 2012). As raw materials for mineral carbonation, natural minerals such as limestone, serpentinite and olivine (Teir et al., 2009; Li et al., 2017; Prigiobbe et al., 2009; Farhang et al., 2016), and various industrial by-products generated in the industry can be used. Recently, industrial by-products with much higher economic advantages than natural minerals are mainly used as raw materials for mineral carbonation. Types of industrial by-products mainly used for mineral carbonation include slag, paper sludge ash, cement kiln dust, fly ash(Polettini et al., 2016; Gunning et al., 2010; Kim et al., 2016; Jo et al., 2012). These industrial by-products contain much metal ions and are in the form of fine particles, which is advantageous for mineral carbonation. Mineral carbonation is generally classified to two: ⅰ) Direct carbonation ⅱ) Indirect carbonation (Fig. 2). The direct carbonation is single process to react carbon dioxide with raw material directly. The direct carbonation does not include the step of eluting metal ions from the raw material prior to carbonation, so the process is simple. Indirect carbonation involves the use of a solvent to elute metal ions from the raw material, and reacting the eluate separated from the raw material with carbon dioxide. In the case of indirect carbonation, impurities such as Si or Fe can be removed to form carbonates of high purity before carbonates are formed. Because the produced $CaCO_3$(s) and $MgCO_3$(s) can be used for industrial purposes, indirect carbonation belongs to CCUS technology (Lackner et al., 1995). For example, calcium carbonate produced via indirect carbonation can be used in the paper, plastics, paint industry, etc (Eloneva et al., 2008).

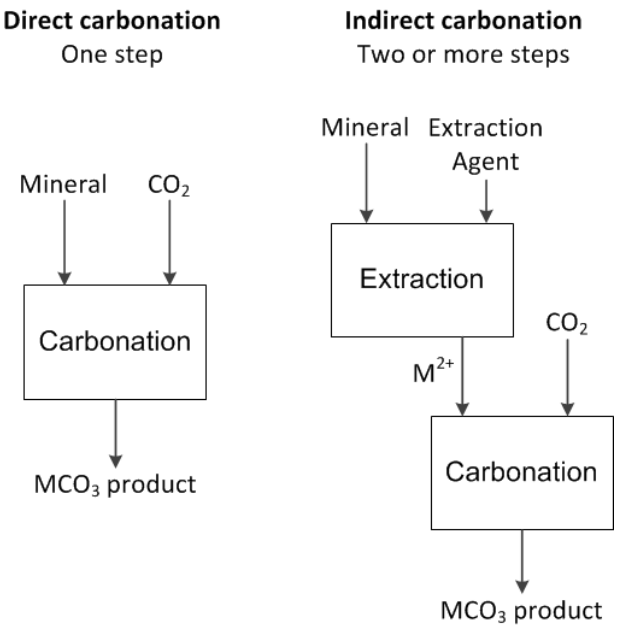

Fig. 2 Direct mineral carbonation is accomplished in one step, while indirect mineral carbonation is conducted in two or more steps. Note M refers to either calcium (Ca) or magnesium (Mg) (Bobicki et al., 2012)

Water, acids (hydrochloric acid, acetic acid, etc.), ammonium salt, and chelating reagents (EDTA, sodium citrate, etc.) have been used as solvents in indirect carbonation (Han et al., 2015; Kim et al., 2017; Zhao et al., 2013; Perez-Moreno et al., 2015; Azdarpour et al., 2015; Mun et al., 2017; Li et al., 2017; Rahmani et al., 2018; Jo et al., 2014; Kim & Kim, 2018). Research has been continued to increase the efficiency of calcium leaching from industrial by-products using various solvents and to increase carbon dioxide storage. In the case of water, the efficiency of eluting Ca from raw materials is low. On the other hand, in the case of acids, the efficiency is considerable; however, a large amount of alkali reagent should be added to increase the pH of the eluate, which has a very low pH. Other solvents have considerable Ca elution ability and high carbonation efficiency and there is no

need to adjust the pH, but the cost of the solvent is high and it is difficult to ensure economic feasibility. Indirect carbonation is technically feasible, but it is difficult to commercialize because of problems of economic feasibility and efficiency. Economic feasibility of the technology is difficult to achieve because chemical solvents account for most of the cost (Azdarpour et al., 2015; Teir et al., 2007). Therefore, in this study, we tried to solve the problems of economic feasibility and efficiency by using nearly costless seawater as a solvent in indirect carbonation.

Meanwhile, Calcium carbonate which is chemically synthesized through these indirect carbonation reactions is precipitated calcium carbonate (PCC). It is classified into calcite, aragonite, and vaterite depending on the form (Chang et al., 2017). Calcite is an rhombohedral shape and is the most stable form of PCC, so it is common. Aragonite is needle-like or orthorhombic particles and it produced under high temperature conditions of 50 to 80 ℃ or higher and in the presence of magnesium ions (Kezuka et al., 2017; Stantos et al., 2014; Altiner & Yildirim, 2017). Vaterite is a spherical particle, which is a metastable form compared to calcite (Brecevic et al., 1996). In the process of PCC formation, amorphous calcium carbonate (ACC) is first generated, and vaterite is produced which is given through the dissolution and recrystallization process of ACC. Also, calcite is formed through the process of dissolution and recrystallization of vaterite (Gebauer et al., 2008; Radha et al., 2010; Rodriguez-Blanco et al., 2010). Vaterite has high specific surface area, high solubility, high dispersibility and low specific gravity rather than calcite and aragonite, and it can be used for various applications than other two forms of calcium carbonate (Trushina et al., 2016).

Seawater contains not only Ca, but also cations, such as Mg^{2+} and K^{+}, and anions, such as HCO_3^{-} and SO_4^{2-} (Table 1). The average concentrations of Ca and Mg are 411 mg/L and 1290 mg/L, respectively (Leggett and Rao, 2015). These are ions that can participate in the carbonation reaction; therefore, seawater is

considered to be advantageous for the production of $CaCO_3$ and $MgCO_3$.

Table 1 Average concentrations of major ions in seawater (Leggett and Rao, 2015)

Component of seawater	Concentration (mg/L)	Concentration (mmol/L)
Cl^-	19000	536.0
Na^+	10800	469.8
SO_4^{2-}	2700	28.1
Mg^{2+}	1290	53.1
Ca^{2+}	411	10.3
K^+	380	9.7
HCO_3^-	140	2.3
Br^-	65	0.8
Sr^{2+}	13	0.1
F^-	0.95	0.05

In this study, various indirect carbonation experiments were conducted using seawater and an alkali industrial by-products. We determined which components of the seawater leached out Ca from the alkali industrial by-products. We determined the optimum conditions of Ca elution and carbonation and compared the CO_2 storage capacity and the $CaCO_3$ yield from this study with previous results. In addition, the influence of seawater on the formation of vaterite-type calcium carbonate was investigated through comparison with existing indirect carbonation reaction solvents. When seawater was used as a solvent, vaterite-type calcium carbonate was produced under various carbonation reaction conditions, and the optimum conditions were derived.

Chapter 2. Indirect mineral carbonation using seawater and alkali industrial by-products

2.1 Materials and Methods

2.1.1 Materials and analysis

The CKD used in this study was supplied from the South Korea “D” cement company, dried at 105 °C for 24 h, and then screened for 425 μm. Seawater was taken from the coastal area in Busan City (South Korea), immediately filtered with a 5 μm paper filter (Filter Paper 2, ADVANTEC), and refrigerated.

Component analysis and pH measurement of the liquid samples were conducted using an atomic absorption spectrometer (AA 200, Perkin Elmer) and pH meter (Orion Star A211, Thermo Fisher Scientific), respectively. Then, in order to determine the components and structure of the solid samples, X-ray diffraction (XRD, Smart lab, Rigaku) analysis, X-ray fluorescence (XRF, XRF-1700, Shimadzu) analysis, thermogravimetric analysis (TGA, TGA 7, Perkin Elmer), and scanning electron microscopy (SEM, MIRA-3, Tescan) analysis were conducted. XRD analysis was conducted at 0.02 ° intervals from 5.0 ° to 80.0 ° at 40 kV/30 mA using CuK-α radiation. TGA was conducted by raising the temperature by 20 °C/min in the range of 50 °C to 900 °C. The particle sizes of the CKD and produced $CaCO_3$ were determined using a laser scattering particle size analyzer (Mastersizer 3000, Malvern Instruments).

2.1.2 Methods

2.1.2.1 Calcium elution reaction

2.1.2.1.1 Calcium elution from CKD using seawater

In order to examine the efficiency of eluting Ca from CKD using seawater as a solvent, CKD and seawater were mixed at a solid/liquid (S/L) ratio of 1:50 (g:mL)

and shaken at 250 rpm and 25 ℃ for 1 h. All reactions that eluted Ca from the CKD were performed at ambient pressure. The suspension was filtered through a 0.45 μm membrane filter and the pH and Ca concentration of the eluate were measured. Ca elution reactions were also conducted under the same conditions using six solvents (distilled water, seawater desalination brine, 0.3 M hydrochloric acid, 0.3 M ammonium chloride, 0.1 M trisodium citrate, and 0.1 M disodium malonate) as a control group. Water, hydrochloric acid, ammonium chloride, and trisodium citrate used in the control group were used as solvents for existing indirect carbonation reactions (Jo et al., 2014; Kim & Kim, 2018; Mun et al., 2017; Teir et al., 2007; Kunzler et al., 2011; Krevor & Lackner, 2009).

2.1.2.1.2 Components of seawater that elutes calcium from CKD

To determine the effective seawater component for Ca elution from CKD, 20 types of artificial solution were prepared and Ca elution experiments were conducted (Table 2). Each artificial solution (solution No. 1-18) was adjusted to contain one to five seawater components each, and the concentration of each ion was adjusted in the same way as that for the average concentration of major ions dissolved in general seawater, as shown in Table 1. The artificial seawater (solution No. 19) was prepared using the method reported by Kester et al. (1967). Other artificial solutions (solution No. 1-18) were also prepared with the same reagents as those used in the artificial seawater preparation method.

The CKD and artificial solution were mixed at a S/L ratio of 1:50 (g:mL) and shaken at 250 rpm and 25 ℃ for 1 h. Then, the suspension was filtered through a 0.45 μm membrane filter and the pH and Ca concentration of the eluate were measured.

Table 2 Composition of artificial solution

1 : HCO_3^-	11 : $Br^- + Cl^-$
2 : SO_4^{2-}	12 : $HCO_3^- + SO_4^{2-} + Br^-$
3 : Br^-	13 : $HCO_3^- + SO_4^{2-} + Cl^-$
4 : Cl^-	14 : $HCO_3^- + Br^- + Cl^-$
5 : Mg^{2+}	15 : $SO_4^{2-} + Br^- + Cl^-$
6 : HCO_3^-+SO_4^{2-}	16 : $HCO_3^- + SO_4^{2-} + Br^- + Cl^-$
7 : HCO_3^-+Br^-	17 : $HCO_3^- + SO_4^{2-} + Br^- + Mg^{2+}$
8 : $HCO_3^- + Cl^-$	18 : $HCO_3^- + SO_4^{2-} + Br^- + Cl^- + Mg^{2+}$
9 : $SO_4^{2-} + Br^-$	19 : artificial seawater
10 : $SO_4^{2-} + Cl^-$	20 : artificial seawater without Mg^{2+}

2.1.2.1.3 Calcium elution using magnesium-added seawater

$MgCl_2 \cdot 6H_2O$ was added to the seawater to adjust the Mg concentration in the seawater to 0.05-0.35 M. CKD and seawater, which adjusted the Mg concentration, were mixed at a S/L ratio of 1:50 (g:mL) and shaken at 250 rpm and 25 ℃ for 1 h. Then, the suspension was filtered through a 0.45 ㎛ membrane filter, and the pH and Ca and Mg concentrations of the eluate were measured.

2.1.2.1.4 The optimal S/L ratio of CKD and seawater

The Ca elution efficiencies according to the S/L ratios were compared by adjusting the ratio of CKD and seawater to 1:25, 1:50, 1:75, 1:100, 1:125, 1:150, and 1:200. For this purpose, 2, 1, 0.67, 0.5, 0.4, 0.33, and 0.25 g of CKD was mixed into 50 mL of seawater, respectively, and shaken at 250 rpm and 25 ℃ for 1 h. Then, the suspension was filtered through a 0.45 ㎛ membrane filter and the pH and Ca concentration of the eluate were measured.

2.1.2.1.5 The optimal reaction temperature and time

Elution experiments were conducted by adjusting the reaction temperature from 0 °C to 80 °C and reaction time from 5 min to 1440 min. For these experiments, the S/L ratio of CKD to seawater was 1:50, and other conditions were the same as those in Section 2.1.2.1.4 The experiment to determine the optimal temperature proceeded at a temperature that was adjusted to be constant in a water bath, and a condenser was installed in the reactor at high temperature ($\geq$ 30 °C) to prevent moisture loss. After completion of the reaction, the pH and Ca concentration of the eluate were measured.

2.1.2.2 Carbonation reaction

The Pyrex reactor (1 L capacity) created for the carbonation reaction had four holes at the top of the reactor for the following purposes (Fig. 3): CO_2 inlet, pH measurement, stirring, and sampling. The CO_2 purity that was used in the reaction was 99.9%. The inside of the reactor was continuously stirred using an electrical stirrer (HS-30D, WISD) while the carbonation reaction progressed.

Experiments were conducted to determine the optimum conditions for three variables (CO_2 flow rate, alkali dosage, and reaction temperature) that could affect carbonation efficiency. In the experiment, the value of the target variable was changed, and the other variables were fixed to the following values: CO_2 flow rate of 2.2 L/min, alkali dosage of 0.0625 M NaOH, and reaction temperature of 25 °C.

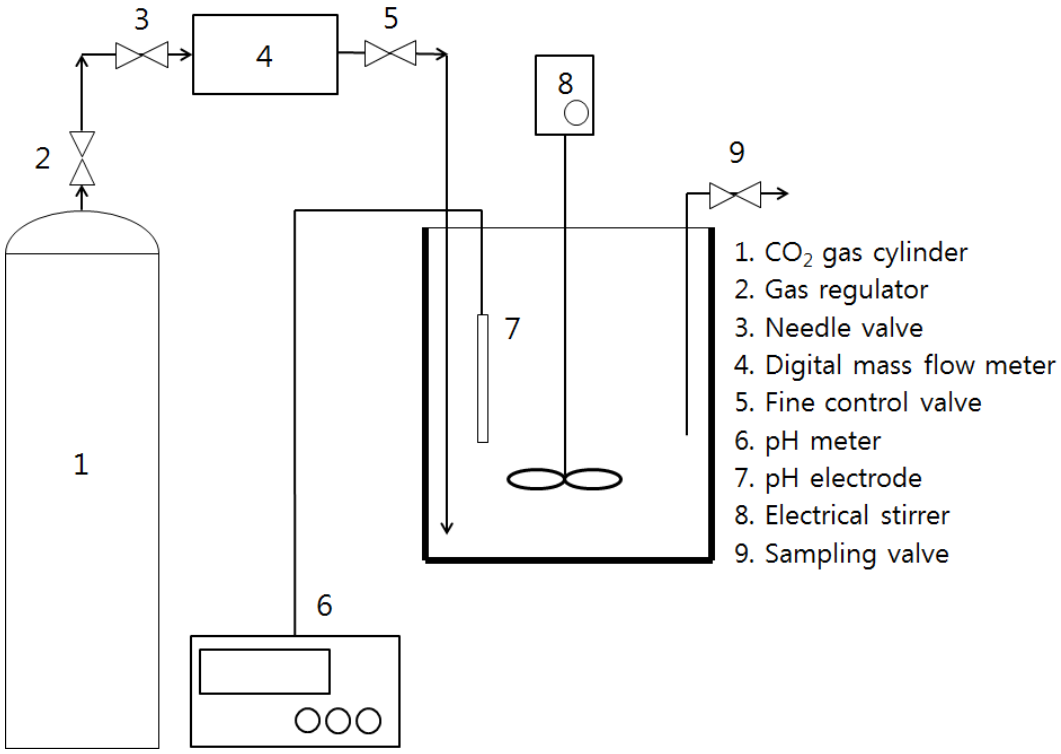

Fig. 3 Schematic of carbonation reactor

2.1.2.2.1 Optimum CO_2 flow rate

CKD and seawater were mixed at a ratio of 1:50 (g:mL), stirred at 250 rpm and 25 °C for 1 h, and then filtered through a 0.45 μm membrane filter to prepare the eluate. Then, 1 L of eluate was added to the reactor and 5 mL of 50% NaOH solution was added to increase the pH of the eluate. This corresponded to 0.0625 M NaOH. The flow rate of CO_2 was adjusted to 0.3, 1.5, 2.2, and 3.0 L/min, respectively, and continuously injected into the eluate for 30 min. The pH of the eluate was continuously monitored and 3 mL of the eluate was sampled at constant time intervals. The eluate was immediately filtered with a 0.45 μm syringe filter (DISMIC-13CP, ADVANTEC), and the Ca concentration of the eluate was measured.

2.1.2.2.2 Optimum alkali addition amounts

To increase the pH of the eluate, 4, 5, 6, and 7 mL of 50% NaOH solution was added to 1 L of eluate. This corresponded to 0.0500, 0.0625, 0.0750, and 0.0875 M NaOH, respectively. The other carbonation conditions were the same as those in Section 2.1.2.2.1.

2.1.2.2.3 Optimum reaction temperature

The carbonation temperature was adjusted to 0, 25, and 80 °C. The other carbonation conditions were the same as those in Section 2.1.2.2.1.

2.1.2.2.4 Analysis of calcium carbonate and calculation of CO_2 storage amount

In order to investigate the morphology, purity, and particle size of $CaCO_3$, we conducted XRD, TGA, SEM, and particle size analysis. All the $CaCO_3$ analyzed was obtained by completing the carbonation reaction at a pH of 10. The $CaCO_3$ was dried at 60 °C for 24 h and used for the analysis. The CO_2 storage and $CaCO_3$ yield were calculated using the difference in Ca concentration of the eluate before and after the carbonation reaction.

The CO_2 storage amounts and $CaCO_3$ yield were calculated by the following equations (1) and (2) using the difference in calcium concentration of the eluate before and after the carbonation reaction.

$$\frac{(C_i - C)}{m_w} \times V \times \frac{MW_{CO_2}}{MW_{Ca}} \qquad (1)$$

$$\frac{(C_i - C)}{m_w} \times V \times \frac{MW_{CaCO_3}}{MW_{Ca}} \qquad (2)$$

herein, C_i : Ca concentration in the eluate before carbonation (mg/L)

C : Ca concentration in the eluate after carbonation (mg/L)

m_w : Mass of CKD used for reaction (g)

V : Eluate volume (L)

MW_{CO_2} : Molar mass of CO_2 (g/mol)

MW_{Ca} : Molar mass of Ca (g/mol)

MW_{CaCO_3} : Molar mass of $CaCO_3$ (g/mol)

2.2 Results and discussion

2.2.1 Analysis of CKD and seawater

As a result of the XRF analysis of the CKD, the Ca and Mg contents were found to be 46.4% and 1.3%, respectively (Table 3). According to the results of the XRD analysis, the Ca of the CKD was mainly present as lime (CaO) (Fig. 4). The pH of the seawater was 8.0, and the concentrations of Ca and Mg were 474 mg/L and 1322 mg/L, respectively. These values were similar to the average values in the literature. Generally, the pH of the surface layer of seawater differs depending on the salt component and concentration, but the average pH is 8.3 and the average concentrations of Ca and Mg are 411 mg/L and 1290 mg/L, respectively (Leggett & Rao, 2015).

Table 3 Chemical compositions of CKD

Composition (wt%)									
CaO	K_2O	Cl	SiO_2	Al_2O_3	MgO	Fe_2O_3	SO_3	Br	TiO_2
46.41	21.02	15.74	6.42	2.32	1.27	1.39	3.65	0.54	0.2

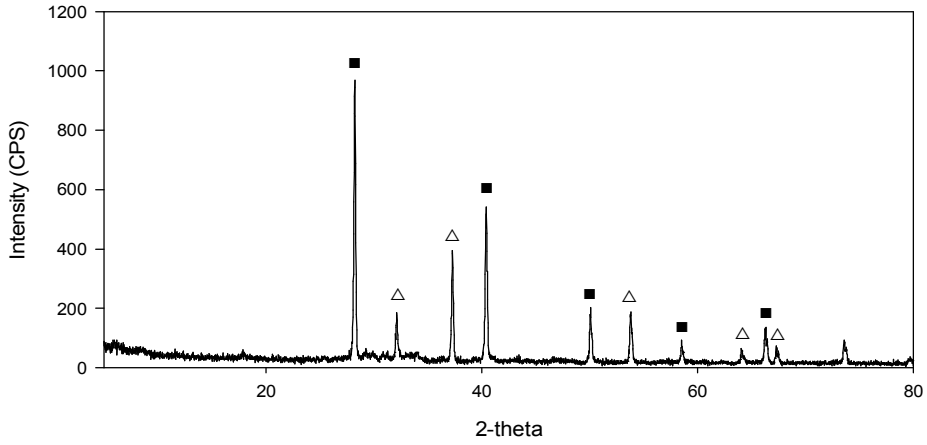

Fig. 4 X-ray Diffraction analysis of CKD (■: Sylvine (KCl), △: Lime(CaO))

2.2.2 Calcium elution reaction

2.2.2.1 Calcium elution from CKD using seawater

The Ca concentration and pH of the eluate obtained using CKD and seawater were 3354 mg/L and 12.5, respectively (Table 4). The Ca elution efficiency was high compared to those of the six solvents used for the control group. The calcium elution efficiency was calculated by the following equation (3).

$$\text{Ca elution efficiency (\%)} = C_i \times \frac{V}{m_w(0.01 \times r_{ca})} \times 100 \quad (3)$$

herein, C_i : Ca concentration eluted from CKD (mg/L)

m_w : Mass of CKD used for reaction (mg)

V : Eluate volume (L)

r_{ca} : Calcium content in CKD (%)

The amount of Ca eluted from the CKD using seawater was more than 2 times as much as that of distilled water. When the seawater desalination brine was used as a solvent, the Ca concentration of the eluate was 3903 mg/L, which was higher than that using seawater. Compared to those using hydrochloric acid, ammonium chloride, and trisodium citrate as existing indirect carbonation solvents, the concentration of Ca eluted using seawater was slightly lower. In this study, however, the fact that seawater could elute Ca at a rate of 3354 mg/L from CKD without using chemical reagents was of great significance. There were two contributing factors that increased the Ca concentration of the eluate obtained by using seawater. First, when Ca eluted from the CKD was precipitated with $Ca(OH)_2$ at a high pH, a large amount of salt present in the seawater converted this to $CaCl_2$ so that more Ca could be eluted (Eq. 4) (Jo et al., 2012). Second, about 400 mg/L of Ca ions that could participate in the carbonation reaction were originally dissolved in seawater.

$$2NaCl(aq) + Ca(OH)_2(s) \rightarrow CaCl_2(aq) + 2NaOH(aq) \quad (4)$$

Table 4 The pH, calcium concentration, and calcium extraction efficiency of the eluate prepared by reaction for the seven solvents with CKD

solvent	Ca concentration (mg/L)	Ca extraction efficiency (%)	pH
seawater	3354	36.1	12.53
desalination brine	3903	42.0	11.44
DI water	1322	14.2	12.99
0.1 M trisodium citrate	4132	44.5	12.98
0.3 M ammonium chloride	5524	59.5	9.92
0.3 M hydrochloric acid	5340	57.5	6.71
0.1 M disodium malonate	1672	18.0	12.82

2.2.2.2 Components of seawater that elutes calcium from CKD

Fig. 5 shows the Ca concentration eluted from the CKD with 20 artificial solutions. When artificial seawater (solution No. 19) was used as a solvent, the Ca concentration and pH of the eluate were 3225 mg/L and 12.2, respectively, and this result was almost the same as that when actual seawater was used as a solvent (Table 3).

It was revealed that Mg had the most significant influence on eluting Ca from CKD among the components of seawater. As shown in Fig. 5, in all cases where the artificial solution containing Mg (solution Nos. 5, 17, 18, and 19) was used, the Ca concentration of the eluate was 2878-3225 mg/L, which was similar to the result when seawater was used. However, when an artificial solution without Mg was used, the Ca concentration of the eluate was 1148-1654 mg/L, which was the same as that when the distilled water was used as a solvent. The Ca elution reaction by Mg could be explained by the following reaction equations (Eqs. 5 and 6):

$$MgCl_2(aq) + CaO(s) + H_2O(l) \rightarrow Mg(OH)_2(s) + CaCl_2(aq) \quad (5)$$

$$Mg(OH)_2(s) \rightarrow Mg^{2+} + 2OH^- \quad K_{sp} = 5.61\times10^{-12} \qquad (6)$$

When the seawater and CKD were mixed, Mg in the seawater precipitated in the form of $Mg(OH)_2$ at a high pH (Fig. 6). This precipitation was considered to be the driving force of the Ca elution reaction (Cho & Kim, 2018).

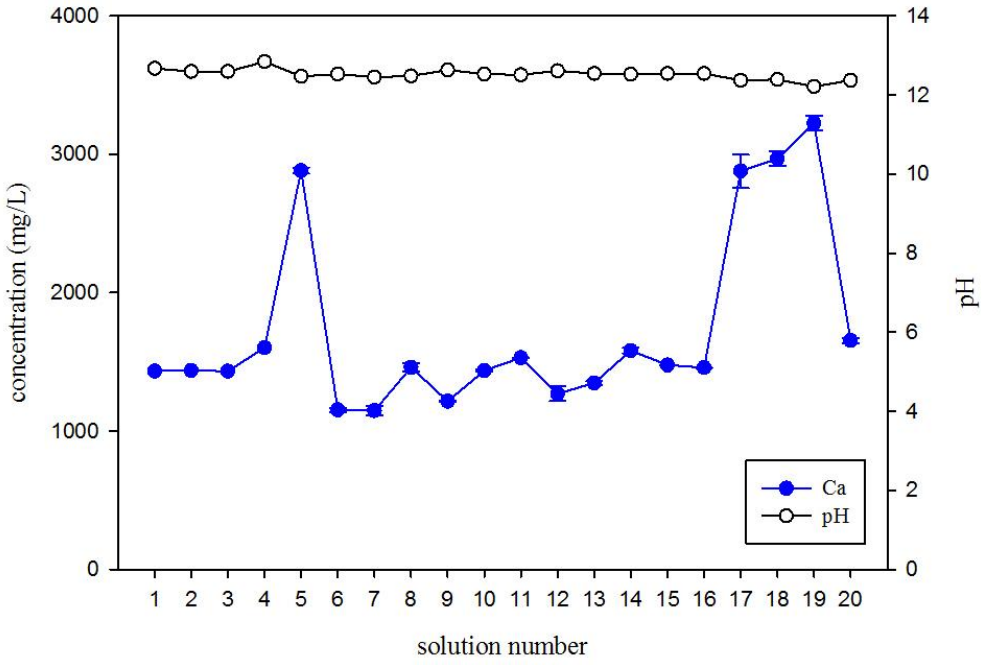

Fig. 5 Ca concentration and pH of eluates obtained using 20 artificial solutions. See Table 2 for details of the solution numbers (horizontal axis)

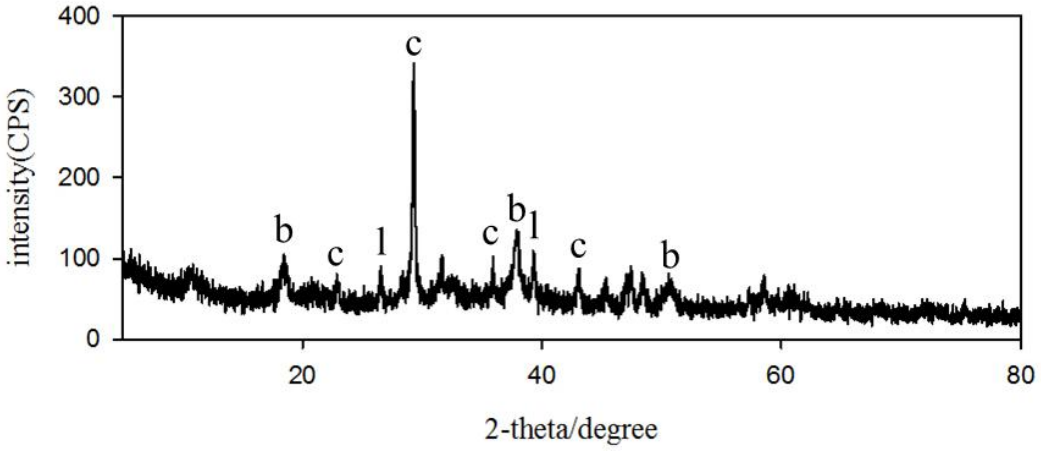

Fig. 6 XRD diagram of solid obtained from the precipitation reaction between CKD and seawater (b: brucite($Mg(OH)_2$), c: calcite($CaCO_3$), l: lime(CaO)).

2.2.2.3 Ca elution using seawater with added Mg

Fig. 7 shows the changes in Ca concentration and pH of the eluate according to the changes in the Mg concentration of the seawater. When the Mg concentration of the seawater was 0.05-0.15 M, the Ca concentration of the eluate continued to increase. For the Mg concentration of the seawater over 0.15 M, the Ca concentration was kept constant at about 5000 mg/L. The changes in the pH of the eluate showed the opposite tendency to changes in the Ca concentration.

The experimental results proved that Mg in seawater plays an important role in the reaction of eluting Ca from industrial by-products. They also showed the possibility of adding Mg to seawater and adjusting the elution amount of Ca.

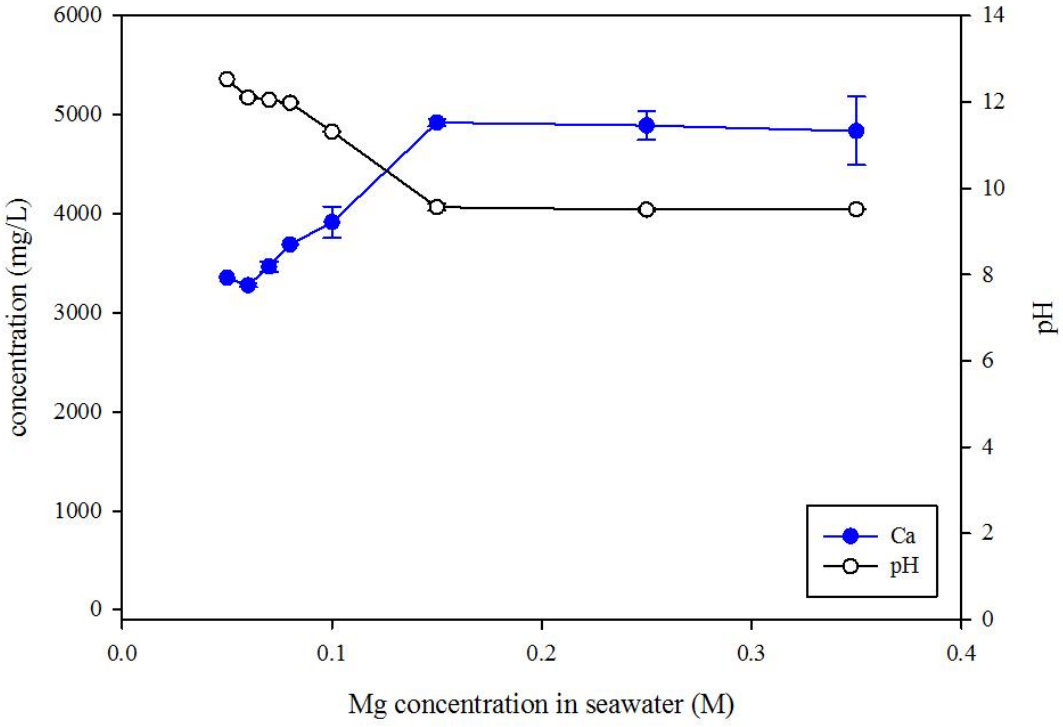

Fig. 7 The change of Ca concentration and pH of the eluate according to the change of Mg concentration in seawater

2.2.2.4 The optimum conditions of the Ca elution reaction

Fig. 8(a) shows the changes in Ca and Mg concentrations and pH of the eluate according to changes in the S/L ratio of the CKD and seawater. As the S/L ratio decreased, the Ca concentration decreased significantly. When the S/L ratio was 1:25 and 1:50, the Ca concentration of the eluate showed a maximum value of 3648 and 3507 mg/L and the pH was high at 12.6 and 12.5, respectively. When the Ca concentration and pH were higher, they were more favorable for the subsequent carbonation reaction (Wang & Maroto-Valer, 2013; He et al., 2013). In

consideration of the amount of CKD, the optimum S/L ratio was determined as 1:50, and the subsequent experiments were conducted under this S/L ratio condition. The Mg concentration of the eluate was 0 mg/L when the S/L ratio was 1:25-1:125.

Fig. 8(b) shows the changes in the Ca concentration and pH of the eluate according to changes in the reaction temperature. With increasing temperature, the Ca concentration of the eluate fluctuated, but overall decreased: see the fitted line in Fig. 8(b). Regardless of the reaction temperature, the pH of the eluate was kept constant at about 12.0-12.2.

According to Jo et al. (2012) the $\Delta H°$ value of the reaction in which Ca is eluted with seawater salt is -17.48 kJ/mol, and this reaction is exothermic ($\Delta H°<0$) (Eq. 7).

$$2NaCl(aq) + CaO(s) + H_2O(l) \rightarrow CaCl_2(aq) + 2NaOH(aq) \quad (7)$$

$$\Delta H°_{Eq.(7)} = -17.48 kJ/mol$$

In addition, the $\Delta H°$ value of the Ca elution reaction by Mg is -79.90 kJ/mol, and this reaction is also exothermic (Eq. 2). These $\Delta H°$ values are consistent with the results shown in Fig. 8(b).

There was almost no change in the Ca concentration and pH of the eluate according to the change in reaction time. That is, even when the elution time varied from 5 min to 1440 min, the concentration of eluted Ca was almost constant because the seawater eluted Ca from the CKD within a short time by precipitation of $Mg(OH)_2$ (Eq.5).

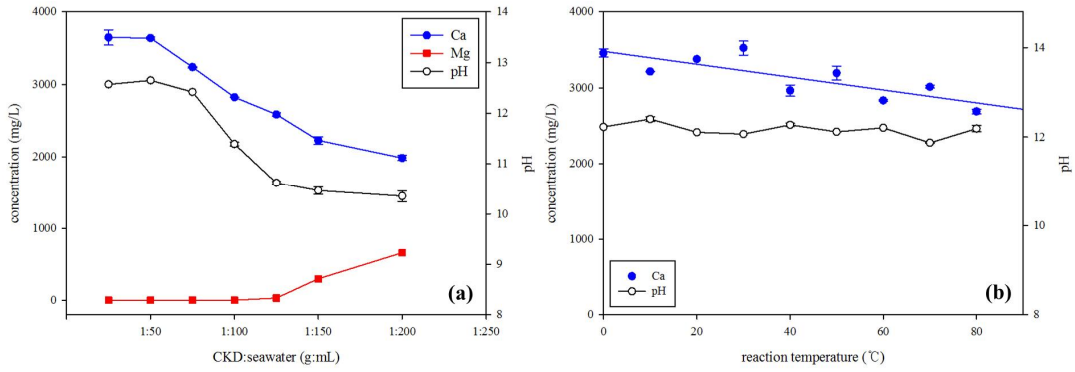

Fig. 8 Variations of Ca and Mg concentrations and pH of eluate according to the changes of (a) S/L ratio, and (b) elution temperature

2.2.2.5 Carbonation reaction

Fig. 9 shows the results of conducting the carbonation reaction by adjusting the CO_2 flow rate and NaOH dosage. When the pH was about 10, the Ca concentration of the eluate was the lowest, which meant that the end-of-carbonation pH at which the carbonation efficiency reached a maximum was about 10. As shown in Fig. 9(a), the higher the CO_2 flow rate, the faster the carbonation reaction rate and the higher the carbonation efficiency. When the CO_2 flow rate was increased from 0.3 L/min to 2.2 L/min, the carbonation completion time (the time when the Ca concentration in the eluate was the lowest) was shortened from 17 min to 6 min. Even though the CO_2 flow rate was increased to 3.0 L/min, the carbonation completion time was also 6 min. Therefore, the optimum CO_2 flow rate was determined to be 2.2 L/min.

The greater the NaOH dosage, the longer the carbonation completion time and the higher the carbonation efficiency (Fig. 9(b)). As the NaOH dosage increased, the time for which the pH of the eluate was maintained above 12 increased, thereby increasing the carbonation efficiency (Eloneva et al., 2008).

When 0.0875 M NaOH was added, more than 99% of the Ca present in the solution was converted to $CaCO_3$.

It was found that the carbonation completion time and efficiency were invariable even when the carbonation temperature was changed to 0-80 °C. Sun et al. (2011) revealed that the influence of temperature on the carbonation rate and carbonation efficiency was not significant when the carbonation reaction progressed at various temperatures using ammonium chloride as a solvent.

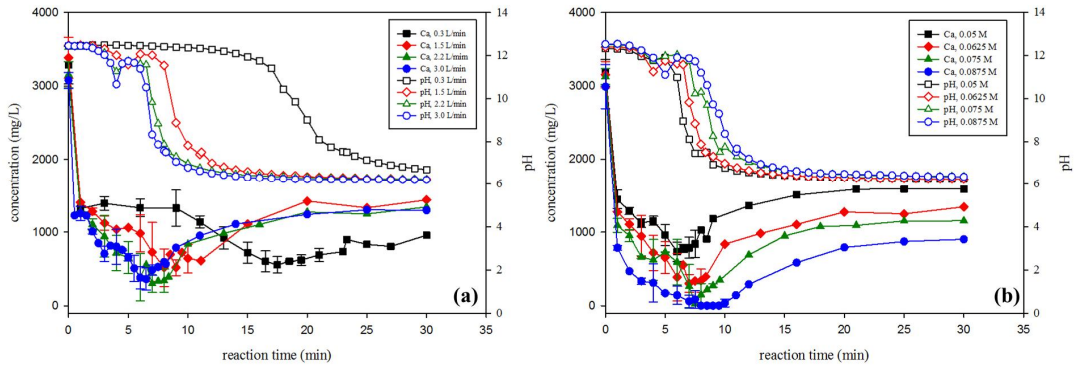

Fig. 9 Variations of Ca concentration and pH during carbonation with (a) CO_2 flow rate (fixed 0.0625 M NaOH) and (b) NaOH dosage (fixed CO_2 flow rate of 2.2 L/min)

2.2.2.6 Properties of the produced $CaCO_3$

Table 5 summarizes the morphology, particle size, and purity of the $CaCO_3$ produced under various carbonation conditions (CO_2 flow rate, alkali dosage, and reaction temperature) using seawater as a solvent. $CaCO_3$ was calcite or vaterite with a purity of 94.6-99.4%, and the particle size was in the range of 2.8-15.7 μm. The calcite and vaterite contents of $CaCO_3$ were calculated using Rao's equation (Rao, 1973). The fraction was calculated using the intensity value of the peak of

each characteristic of calcite and vaterite (Fig. 10). Calculation equations are as follows (Eqs. 8 and 9).

$$f(v) = \frac{I_{100} + I_{101} + I_{102}}{I_{100} + I_{101} + I_{102} + 0.43 \times I_{104}} \times 100 \quad (8)$$

$$f(c) = 100 - f(v) \quad (9)$$

In the above equation, $f(v)$ and $f(c)$ indicate the ratio of vaterite and calcite, respectively. I_{100}, I_{101}, and I_{102} are vaterite characteristic peak intensity values on the XRD graph, and I_{104} is the intensity value of the calcite characteristic peak. I_{100}, I_{101}, and I_{102} exist near the 2-theta values of 24.81 °, 27.09 °, and 32.75 °, respectively, and in the case of I_{104}, they exist in the vicinity of 29.32 °.

Table 5 Morphology, particle size and purity of $CaCO_3$ produced under various carbonation conditions

Variable	sample notation	Carbonation conditions			carbonation completion time (min)	$CaCO_3$ morphology		$CaCO_3$ median particle size, D50 (μm)	weight reduction at 500-820 °C for TGA (%)	$CaCO_3$ purity (%)
		CO_2 flow rate (L/min)	NaOH dosage (M)	temperature (°C)		calcite (%)	vaterite (%)			
CO_2 flow rate	A	0.3	0.0875	25	20.3	100	0	3.4	43.2	98.1
	B	1.5	0.0875	25	10.5	100	0	6.6	43.0	97.8
	C	2.2	0.0875	25	8.5	15.8	84.2	4.6	42.9	97.6
	D	3.0	0.0875	25	7.9	34.3	65.7	5.7	42.7	97.1
NaOH dosage	E	2.2	0.0625	25	7.0	2.3	97.7	4.1	41.6	94.6
	F	2.2	0.0750	25	8.2	17.3	82.7	4.9	42.7	97.0
	G	2.2	0.0875	25	8.5	15.8	84.2	4.6	42.9	97.6
Temperature	H	2.2	0.0875	0	8.5	35.3	64.7	15.7	43.8	99.4
	I	2.2	0.0875	25	8.5	15.8	84.2	4.6	42.9	97.6
	J	2.2	0.0875	80	8.5	100	0	2.8	43.0	97.8

When carbonation was conducted, the higher the CO_2 flow rate (C, D) and the lower the NaOH dosage (E), the more vaterite-type $CaCO_3$ was produced. In other words, the shorter the carbonation completion time, the more vaterite was produced. For instance, when the CO_2 flow rate was as low as 0.3-1.5 L/min (A, B), 100% calcite was produced. When the CO_2 flow rate was above 2.2 L/min (C, D), $CaCO_3$ containing 65.7-84.2% vaterite was produced. Also, when the NaOH dosage was adjusted to 0.0625-0.0875 M (E, F, G), $CaCO_3$ mixed with calcite and vaterite was produced in all cases. When the NaOH dosage was the lowest at 0.0625 M, $CaCO_3$ with the highest vaterite content (97.7%) was produced. This result can be explained as follows. At the beginning of the carbonation reaction, amorphous

calcium carbonate was first formed and rapidly transformed into vaterite. Vaterite formed in this way was transformed into calcite through dissolution and recrystallization (Rodriguez-Blanco et al., 2011). That is, because the vaterite-type $CaCO_3$ was in a very metastable form, when the carbonation time increased, it was transformed into calcite form.

When the carbonation temperature was adjusted to 0-80 °C (H, I, J), the particle size of $CaCO_3$ decreased significantly as the temperature increased. It was 15.7 μm and 2.8 μm at 0 °C and 80 °C, respectively. At 80 °C, 100% calcite was formed, whereas at 0-25 °C, vaterite and calcite were mixed.

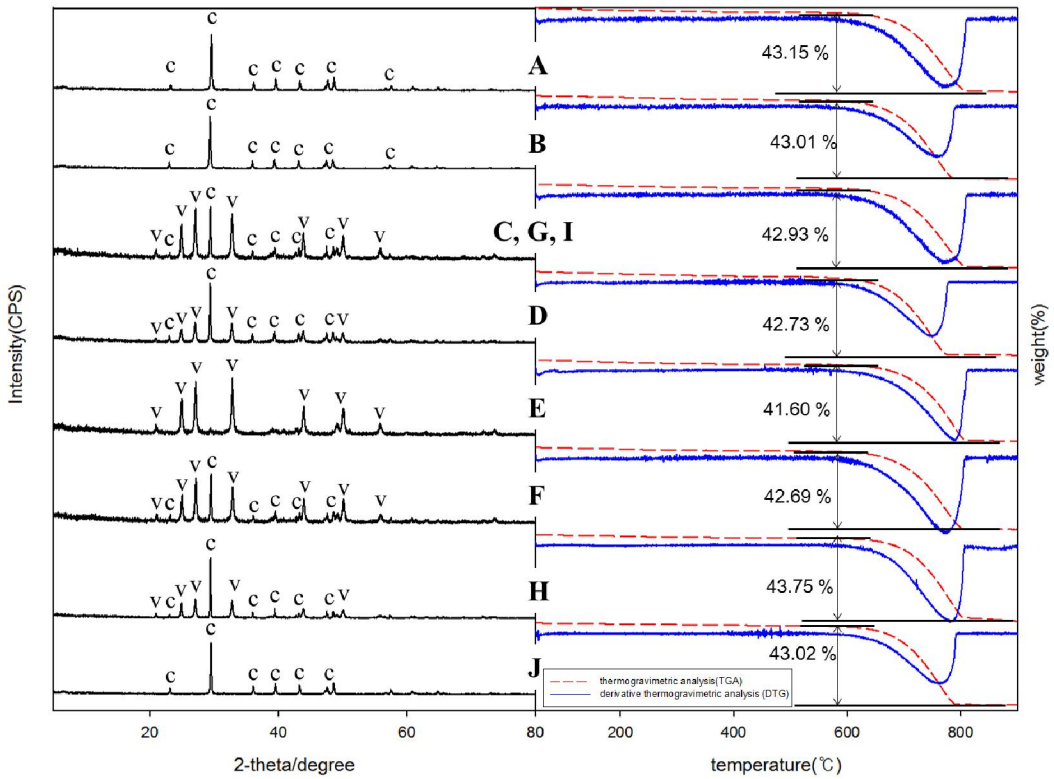

Fig. 10 XRD and TGA/DTG of $CaCO_3$ produced under various carbonation conditions (c: calcite, v: vaterite, --- TGA, — DTG)

The purity of $CaCO_3$ calculated using TGA was greater than 94.6% in all the experimental conditions (Table 5) (Huntzinger et al., 2009; Villain et al., 2007; Bouquet et al., 2009). The differential thermogravimetry (DTG) graph (solid line) in Figure 7 shows a single large valley in the range of 500-820 °C and no valley at other temperatures. This result indicated that even if CKD and seawater, which contain a large amount of impurities, are used as the raw material and solvent, respectively, no carbonate solids of other metal ions are produced and only $CaCO_3$ is produced (Jazairi, 1977).

It was confirmed by SEM that the shape of $CaCO_3$ changed according to the NaOH dosage and carbonation temperature (Fig. 11). When the NaOH dosage was as low as 0.0625 M (E), only the spherical vaterite was clearly shown. On the other hand, as the NaOH dosage increased (F, G), the rhombohedral calcite increased. Meanwhile, the shapes of calcite and vaterite appeared differently depending on the carbonation temperature. Of the $CaCO_3$ produced at 0 °C (H), calcite existed as single particles with a rhombohedral shape and vaterite existed in the shape of broccoli rather than spheres. The $CaCO_3$ produced at 25 °C (I) consisted of rhombohedral calcite and spherical vaterite. At 80 °C (J), 100% calcite was produced, and the shape of the calcite was rod-like rather than rhombohedron.

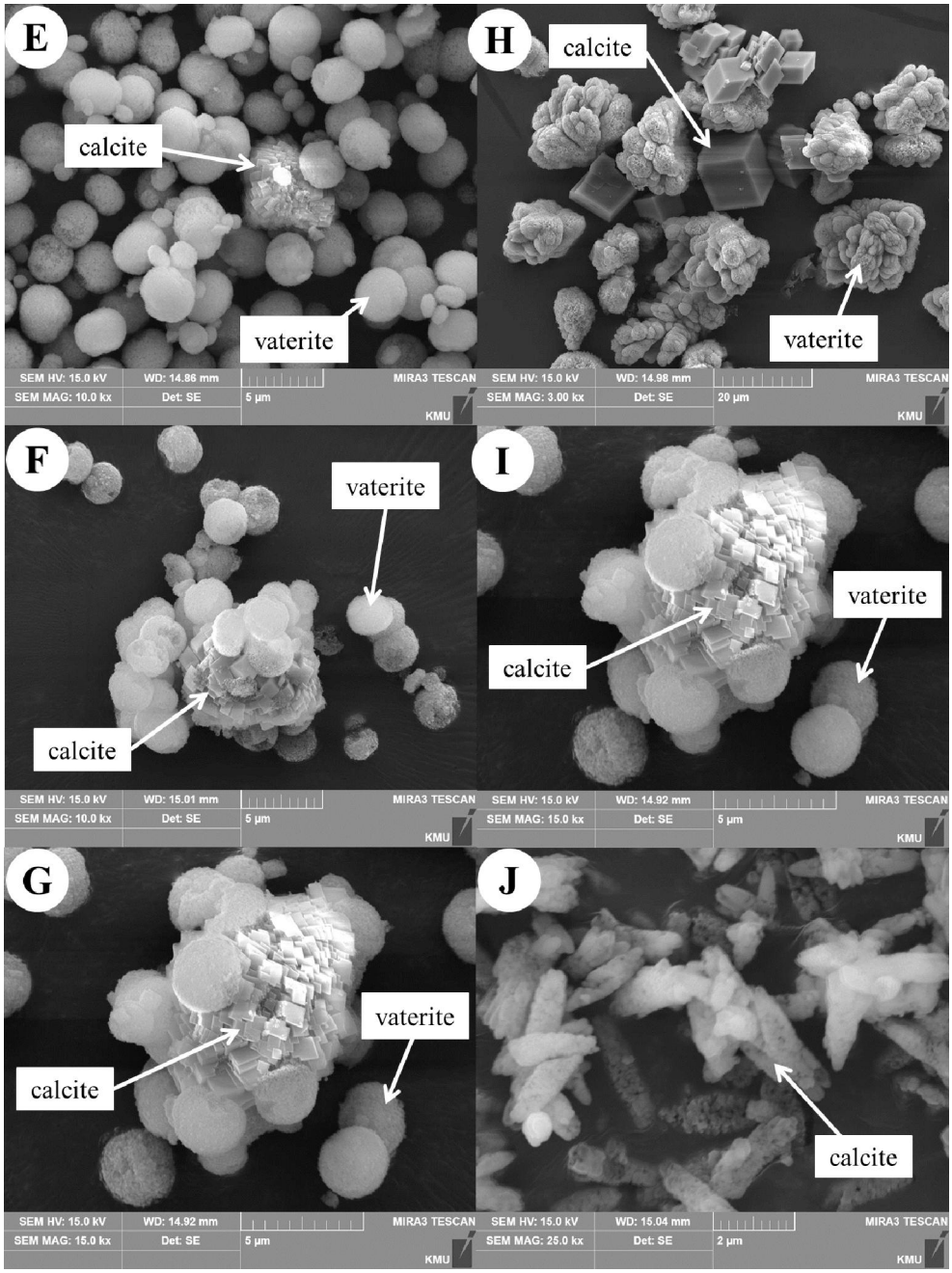

Fig. 11 SEM images of $CaCO_3$ produced under various carbonation conditions. See Table 5 for detail conditions

2.2.2.7 CO_2 storage amounts and $CaCO_3$ yield

The CO_2 storage amounts and $CaCO_3$ yield under the following optimal conditions were 185 kg-CO_2/ton-CKD and 419 kg-$CaCO_3$/ton-CKD, respectively (Table 6). The optimal S/L ratio of the Ca elution reaction was 1:50. The optimal conditions for the carbonation reaction were a CO_2 flow rate of 2.2 L/min, NaOH dosage of 0.0875 M, and end-of-carbonation pH of 10. When the Mg concentration of seawater increased to 0.15 M, the CO_2 storage amounts and $CaCO_3$ yield increased to 271 kg-CO_2/ton-CKD and 615 kg-$CaCO_3$/ton-CKD, respectively. Table 5 shows the extracted Ca concentration, CO_2 storage amounts, and $CaCO_3$ yield from the previous studies using ammonium salts and hydrochloric acid as well as those from this study using seawater. As shown in Table 5, the CO_2 storage amounts and $CaCO_3$ yield in this study were much larger than those obtained in most previous studies, except for some results using acid.

The Ca concentration of the eluate obtained in this study was 3354-4922 mg/L. This was similar to the values obtained by Jo et al. (2014) and Kim and Kim (2018) for a S/L ratio of 1:50. However, the CO_2 storage amounts and $CaCO_3$ yield per ton of industrial by-products obtained in this study were greater than those obtained in the previous two studies. The reason for this was that the S/L ratio of the industrial by-product and seawater was 1:50, which was much lower than that of previous studies (Jo et al., 2014). The difference in carbonation efficiency could also be a factor (Kim and Kim, 2018).

In this study, by using seawater and CKD, it was possible to store more CO_2 and produce more $CaCO_3$ than those in previous studies, thereby making indirect carbonation technology more environmentally friendly and economical. In addition, by using nearly costless seawater instead of chemical reagents as an indirect carbonation solvent, this study reduced the solvent cost that accounts for the largest part of the production cost of technology to nearly 0. This will greatly improve the economics of the technology.

Table 6 Extracted Ca concentration, CO_2 storage, and $CaCO_3$ yield from the previous studies as well as this study

	raw material	solvent	S/L ratio	extracted Ca concentration (mg/L)	CO_2 storage amounts (kg-CO_2/ton-waste)	$CaCO_3$ yield (kg-$CaCO_3$/ ton-waste)	reference
This study	CKD	seawater	1:50	3354	184.5	419.3	
		seawater (Mg conc. 0.15 M)	1:50	4922	270.7	615.3	
Previous study	waste cement	0.50 M NH_4Cl	1:20	2479	45.3	102.9	Jo et al. (2014)
		1.00 M NH_4Cl	1:20	4079	69.6	158.2	
	paper sludge ash	0.70 M CH_3COOH	1:25	13052	324.0	736.4	Kim and Kim (2018)
		0.70 M HCl	1:25	13124	297.0	675.0	
		0.30 M NH_4Cl	1:50	4450	175.0	397.7	
		0.30 M NH_4CH_3COO	1:50	4080	135.0	306.8	
		0.30 M sodium citrate	1:50	4283	136.0	309.1	
		water	1:50	1068	29.1	66.1	
	waste cement	0.50 M HCl	1:10	13670	190	431.8	Mun et al. (2017)
		0.50M CH_3COOH	1:10	13220	190	431.8	
		0.50 M NH_4Cl	1:10	6733	70	159.1	
	steel slag	0.29-2.00 M HCl	1:10	2800	127.8	290.5	Kunzler et al. (2011)

2.3 Conclusions

In most previous studies, Ca was removed in the form of $CaCO_3$ to suppress the scale generated in processes using seawater. However, in this study, the first attempt was made to store CO_2 and simultaneously produce $CaCO_3$ using seawater. Mg was found to be a component of seawater that eluted Ca from alkali industrial

by-products, and the optimum conditions to increase the efficiencies of both Ca elution and carbonation were derived. By using nearly costless seawater and CKD, the production of $CaCO_3$ with a purity of 99.4% was increased to 615 kg-$CaCO_3$/ton-CKD, thereby remarkably improving the economic feasibility of indirect carbonation technology. If cement manufacturing plants or paper mills that discharge large amounts of CO_2 and use $CaCO_3$ as a raw material are in close proximity to the ocean, then this technology could be applied to reduce CO_2 emissions and reuse the produced $CaCO_3$ in the industrial process. We expect that it will be possible to operate an eco-friendly and economical resource recycling plant.

Chapter 3. Method of vaterite type calcium carbonate production using seawater and alkali industrial by-products

3.1 Materials and Methods

3.1.1 Materials and analysis

The raw materials used in this study were cement kiln dust (CKD) and paper sludge ash (PSA) which are alkali industrial by-products. In addition, CaO and $Ca(OH)_2$ that chemical reagent were also used. CKD and PSA was supplied from the South korea “D” cement company and South Korea “A” paper-mill respectively, dried at 105 °C for 24 h, and then screened for 425 μm. CaO purchased from Hayashi Pure Chemical Ind. (Assay min. 98 %) and $Ca(OH)_2$ purchased from Junsei Chemical (Assay min. 96 %).

The solvents for the indirect carbonation reaction used seawater and seawater desalination brine. Seawater was taken from the coastal area in Busan City (South Korea), and seawater desalination brine supplied from South Korea ‘A’ seawater desalination plants (Na & Kim, 2019). They immediately filtered with a 5 μm paper filter (Filter Paper 2, ADVANTEC), and refrigerated.

In order to determine the components and structure of the solid samples, X-ray diffraction (XRD, Smart lab, Rigaku) analysis, X-ray fluorescence (XRF, XRF-1700, Shimadzu) analysis, and scanning electron microscopy (SEM, SUPRA-40VP, ZEISS) analysis were conducted. XRD analysis was conducted at 0.02 ° intervals from 5.0 ° to 80.0 ° at 40 kV/30 mA using CuK-α radiation. The particle sizes of the CKD and produced $CaCO_3$ were determined using a laser scattering particle size analyzer (Mastersizer 3000, Malvern Instruments). Component analysis and pH measurement of the liquid samples were conducted using an atomic absorption spectrometer (AA 200, Perkin Elmer) and pH meter (Orion Star A211, Thermo Fisher Scientific), respectively.

3.1.2 Method

3.1.2.1 Calcium elution reaction using seawater

Experiment was conducted to determine the S/L ratio that elutes the most calcium from industrial by-products as follows. To adjust the S/L ratio of CKD to seawater (g:mL) to 1: 5, 1:10, 1:25, 1:50, mixing CKD 10, 5, 2, 1 g with 50 mL of seawater respectively and it stirred at 25 °C and 250 rpm for 1 hour. After stirring was over, the suspension was filtered through a 0.45 μm membrane filter (MCE04547A, HYUNDAI Micro Co,), and the calcium concentration and pH of the eluate were measured. The same experiment was conducted with PSA, calcium oxide, calcium hydroxide instead of CKD, and with seawater desalination brine instead of seawater.

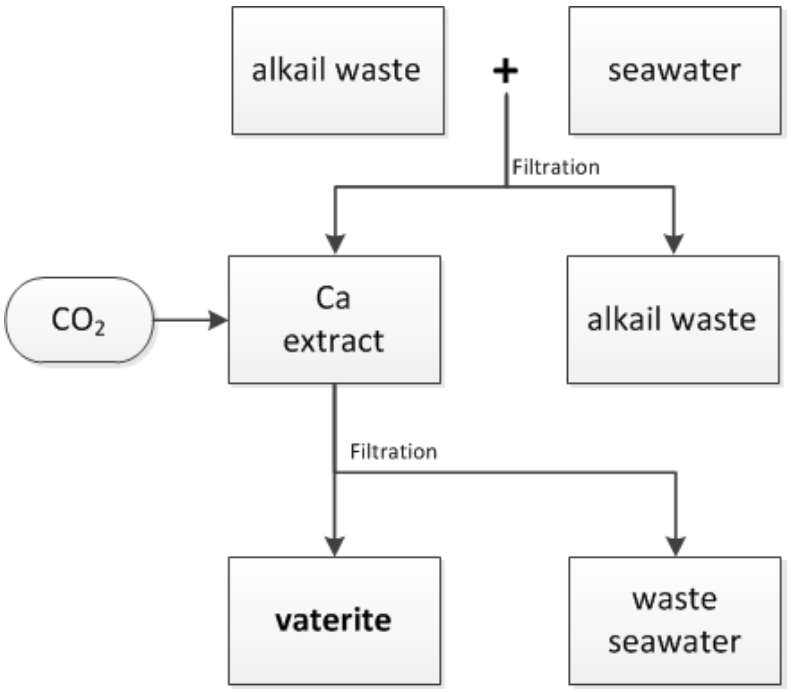

Fig. 12 Processes to produce vaterite type calcium carbonate using seawater

3.1.2.2 Vaterite formation via carbonation reaction

The Pyrex reactor (1 L capacity) created for the carbonation reaction had four holes at the top of the reactor for the following purposes (Fig. 3): CO_2 inlet, pH measurement, stirring, and sampling. Stirring at a constant speed using a stirrer (HS-30D, WISD), the pH was measured in real time using a pH meter. The carbon dioxide flow rate was measured and adjusted using a gas flow meter and flow controller (TSM-D220, MKP).

3.1.2.2.1 Effects of seawater on vaterite formation

The calcium elution reaction and the carbonation reaction were carried out under the same conditions using seawater and four existing widely used solvents, and then the forms of calcium carbonate produced were compared. The solvents mainly used for the indirect carbonation reaction up to now are acids (hydrochloric acid, acetic acid etc.), ammonium salts (ammonium chloride, ammonium acetate etc.), chelating agents, and distilled water (Han et al., 2015; Kim et al., 2017; Zhao et al., 2013; Perez-Moreno et al., 2015; Azdarpour et al., 2015; Mun et al., 2017; Li et al., 2017; Rahmani et al., 2018; Jo et al., 2014; Kim & Kim, 2018). Among these, 0.3 M HCl, 0.3 M NH_4Cl, 0.1 M $C_3H_2Na_2O_4$ and distilled water were selected, and a total of five solvents including seawater were used.

CKD and each solvent were mixed at a ratio of 1:50 (g: mL), stirred at 250 rpm for 1 hour, and then filtered to prepare 1 L of calcium eluate.In the case of seawater and 0.3 M HCl, the pH was raised by adding 5 mL of 50% aqueous NaOH solution before injecting carbon dioxide. While stirring the calcium eluate at 300 rpm, it was carbonated by injecting 99.9% carbon dioxide at a flow rate of 3.0 L / min. At this time, the diameter of the stirring impeller was 70 mm. After completing the carbonation reaction, the carbonate was filtered through a 0.45 μm membrane filter, dried at 60 °C. for 24 hours and analyzed.

3.1.2.2.2 Effects of seawater type and raw material on vaterite formation

The calcium elution reaction and the carbonation reaction were performed using PSA, CaO, $Ca(OH)_2$ and seawater desalination brine instead seawater and CKD. The experimental conditions and method were the same as section 3.1.2.2.1.

3.1.2.2.3 Influence of carbonation reaction conditions on vaterite formation

When seawater was used, the carbonation reaction proceeded under various conditions according to the impeller diameter and stirring speed, and the influence of each carbonation reaction condition on the formation of vaterite was investigated. The diameters of the used impellers were 50 mm and 70 mm, and the stirring speed was adjusted at 300 to 800 rpm. Other experimental conditions and methods were the same as section 3.1.2.2.1. However, the solvent used seawater.

3.2 Results and discussion

3.2.1 Analysis of industrial by-products and seawater

CKD is a by-product generated in the cement production process, and PSA is a by-product generated when incinerating papermaking sludge. The calcium content of CKD and PSA was very high at 46.4% and 69.5%, respectively. According to the results of XRD analysis, calcium of CKD was mainly present in lime (CaO) and calcium of PSA was present in the form of portlandite ($Ca(OH)_2$), lime (CaO) and calcite ($CaCO_3$) (Fig. 13). The median particle sizes of CKD and PSA were 23.6 μm and 126.9 μm, respectively. Not only are CKD and PSA fine and do not need to be crushed, they are also highly suitable raw materials for the carbonation reaction because of their high calcium content.

The pH of seawater used in this study was 7.97, and the concentrations of calcium and magnesium were 474 mg/L and 1322 mg/L, respectively. This value is similar to the average value of the literature. Generally, the pH of surface seawater

is 8.3 on average, and the average concentrations of calcium and magnesium are 411 mg/L and 1290 mg/L, respectively, although it varies depending on the composition and concentration of salt. The pH of seawater desalination brine was 7.80, which was similar to that of seawater, and the concentrations of calcium and magnesium were 664 mg/L and 2340 mg/L. It is 1.6 to 1.8 times higher than seawater.

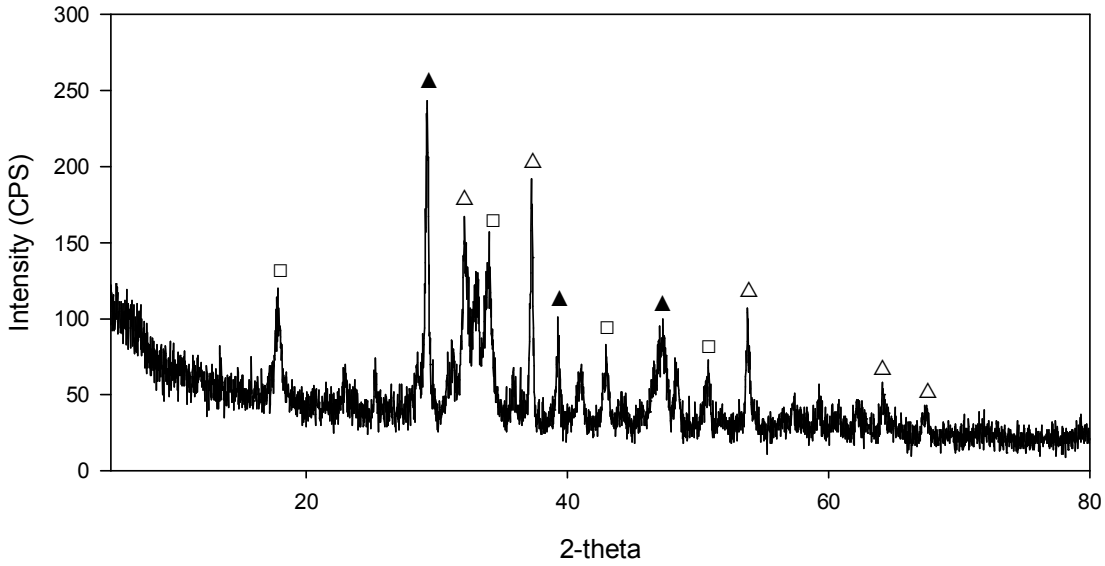

Fig. 13 X-ray Diffraction analysis of PSA (□: Portlandite ($Ca(OH)_2$), △: Lime (CaO), ▲: Calcite ($CaCO_3$))

3.2.2 Calcium elution reaction using seawater

In indirect carbonation reaction, the calcium concentration and pH of the eluate are important factors to determine the efficiency of carbonation reaction. The more calcium is eluted from raw materials such as industrial by-products, and the higher pH of the eluate favors the carbonation reaction (He et al., 2013; Wang & Maroto-Valer, 2013). Changes in calcium concentration and pH of the eluate due to

S/L ratio changes in raw materials and solvents are shown in Table 7 and Fig. 14.

The higher S/L ratio of industrial by-products and seawater, the higher the calcium concentration and the lower the pH. The calcium concentration of the eluate was the highest when the high price ratio was 1:25-1:50, and the maximum calcium concentration was 3648 mg/L and 2532 mg/L when using CKD and PSA, respectively. The pH of the eluate was all over 11.9. When seawater desalination brine was used as a solvent, the calcium concentration eluted from CKD was slightly higher and pH was lower at 11.4 than when seawater was used. Seawater and sewater desalination brine contains large amounts of salt and magnesium. When Ca eluted from the CKD was precipitated with $Ca(OH)_2$ at a high pH, a large amount of salt converted this to $CaCl_2$ (Eq. 10). And, more calcium can be eluted through the precipitation reaction of magnesium (Eqs. 11 and 12), so that more Ca could be eluted.

$$2NaCl(aq) + Ca(OH)_2(s) \rightarrow CaCl_2(aq) + 2NaOH(aq) \quad (10)$$

$$MgCl_2(aq) + Ca(OH)_2(s) \rightarrow Mg(OH)_2(s) + CaCl_2(aq) \quad (11)$$

$$Mg(OH)_2(s) \rightarrow Mg^{2+} + 2OH^- \quad K_{sp}=5.61\times10^{-12} \quad (12)$$

Therefore, since seawater desalination brine is higher salinity and higher magnesium concentration than general seawater, it is possible to elute more calcium than general seawater. However, the pH was relatively low due to the loss of OH^- ions due to the large amount of magnesium precipitated.

When seawater was used as a solvent and CaO and $Ca(OH)_2$ were used as raw materials, the calcium concentration was 3692 and 2876 mg / L, respectively, and the pH was 12.52 and 12.41 respectively, similar to when industrial by-products were used.

Table 7 The calcium concentration and pH of eluent according to seawater and various raw materials

raw material	solvent	S/L ratio (g/mL)	Ca concentration (mg/L)	pH
CKD	seawater	1:5	2572.5	12.67
		1:10	3321.5	12.61
		1:25	3647.5	12.57
		1:50	3507	12.53
	seawater desalination brine	1:50	3903	11.44
PSA	seawater	1:5	1819.5	12.6
		1:10	2324	12.57
		1:25	2465.5	12.5
		1:50	2532	11.92
CaO	seawater	1:10	3692	12.52
$Ca(OH)_2$	seawater	1:10	2876	12.41

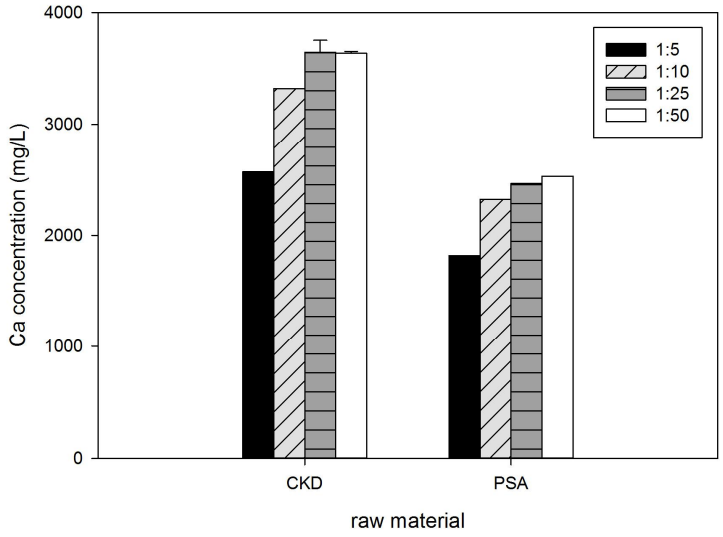

Fig. 14 Variations of the calcium concentration of eluent with the S/L ratio each industrial by-products

3.2.3 Vaterite formation via carbonation reaction

3.2.3.1 Effects of seawater on vaterite formation

Size, shape and $CaCO_3$ yield through indirect carbonation reaction using CKD and five solvents (seawater, distilled water, 0.1 M $C_3H_2Na_2O_4$, 0.3 M HCl, 0.3 M NH_4Cl) are summarized in Table 8. The $CaCO_3$ yield produced was calculated as the change in calcium concentration before and after the carbonation reaction.

The calcium carbonates produced using five solvents, including seawater, were vaterite and calcite. When seawater was used as a solvent for the indirect carbonation reaction, the content of vaterite of calcium carbonate produced was 100%, and the content of vaterite was much higher than that of other solvents. As a result of XRD analysis of calcium carbonate produced for each solvent, only the vaterite peak was confirmed when seawater was used as a solvent, and all vaterite and calcite peaks were confirmed when a solvent other than seawater was used (Fig. 15). This result indicates that seawater is a very advantageous solvent for producing vaterite by indirect carbonation reaction.

The calcite and vaterite content of calcium carbonate produced was calculated by RaO's equation, and the fractions were calculated using the intensity value of the peak of each property of calcite and vaterite (Rao, 1973).

Unlike distilled water, the precipitation reaction of calcium carbonate from seawater does not occur easily. Chemical precipitation of calcium carbonate from seawater requires a high concentration to reach 18 times the saturation concentration of calcium carbonate, but in fact, the calcium carbonate concentration in surface ocean water is about 4 to 6 times the saturation concentration, so precipitation does not occur well (Morse & He, 1993). Thus, despite the fact that calcium carbonate is supersaturated from seawater, the reason is not solved because

ions such as Mg^{2+}, PO_4^{3-}, Cl^- and SO_4^{2-} interfere with calcium carbonate nucleation.

In this study, vaterite was generated through indirect carbonation reaction using seawater and alkaline industrial by-products. It is thought that it has acted favorably in producing metastable vaterite given the conditions in which calcium carbonate nucleation is difficult from seawater. Previous studies to produce Vaterite use additives such as MEG, NH_4OH, or use processes that generate additional costs such as ultrasound. (Han et al., 2006; Marie et al., 2010; Chen et al., 2017, Price et al., 2011). However, In this research, it is extremely advantageous in terms of the economics of the technology to produce vaterite using low cost or free sea water as a solvent, starting from alkali industry by-products continuously generated in the industry.

The particle size of calcium carbonate produced using seawater was 2.29 μm, which is much smaller than when using other solvents. In addition, when seawater was used as a solvent the amount of $CaCO_3$ (vaterite) yield was 341 kg / ton-CKD. It is more than when other solvents were used.

Table 8 Morphology, particle size and yield of $CaCO_3$ produced using five solvents that include seawater

solvent	S/L ratio (g/mL)	$CaCO_3$ morphology		$CaCO_3$ median particle size, D_{50} (μm)	$CaCO_3$ yield (kg/ton-CKD)
		vaterite (%)	calcite (%)		
Seawater	1:50	100	0	2.29	341
DI water		14.2	85.8	7.24	139
0.1 M $C_3H_2Na_2O_4$		74.0	26.0	11.49	190
0.3 M HCl		44.8	55.2	10.38	607
0.3 M NH_4Cl		42.8	57.2	15.39	514

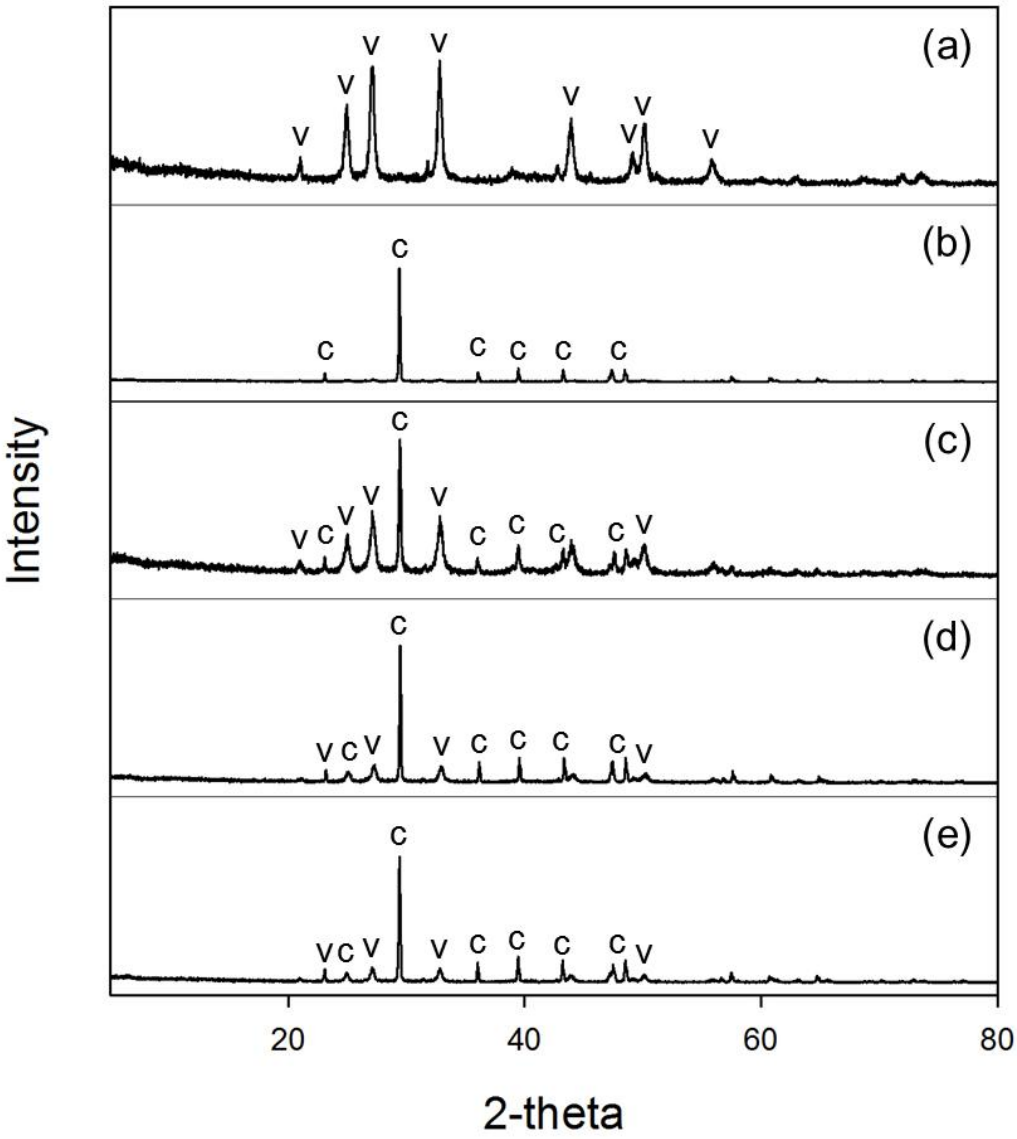

Fig. 15 XRD analysis of the $CaCO_3$ produced using five solvents that include seawater: (a) seawater, (b) DI water, (c) 0.1 M $C_3H_2Na_2O_4$, (d) 0.3 M HCl, (e) 0.3 M NH_4Cl

3.2.3.2 Effects of seawater type and raw material on vaterite formation

As shown in Table 9, 100% vaterite was produced when using the seawater desalination brine instead of seawater. And when seawater was used as a solvent, regardless of the raw materials (CKD, PSA, CaO, $Ca(OH)_2$), the produced calcium carbonate was almost 100% vaterite. The particle size of the calcium carbonate produced was 2.29-5.27 μm and the purity was high up to 97.4%. This result indicates that calcium carbonate having a high content of vaterite can be produced regardless of the type of seawater and the type of raw material. Fig. 16 and Fig. 17 are the results of XRD and SEM analysis of calcium carbonate prepared using seawater and seawater desalination brine, respectively. This result uses the seawater and seawater desalination brine to prove that nearly 100% vaterite-type calcium carbonate is produced in all cases. On the other hand, the vaterite-type calcium carbonate produced when seawater was used showed a spherical form, but the vaterite-type calcium carbonate produced when seawater desalination brine was elliptical form. Oral and Ercan (2018) reported that elliptical vaterite perform high reactivity than spherical vaterite.

Table 9 Morphology, particle size and purity of $CaCO_3$ produced using seawater and various raw materials

raw material	solvent	$CaCO_3$morphology		$CaCO_3$ median particle size, D_{50} (μm)	purity (%)
		vaterite (%)	calcite (%)		
CKD	seawater	100	0	2.29	96.50
	seawater desalination brine	100	0	4.22	97.41
PSA	seawater	97.0	3.0	5.27	95.73
CaO	seawater	100	0	-	-
$Ca(OH)_2$	seawater	100	0	-	-

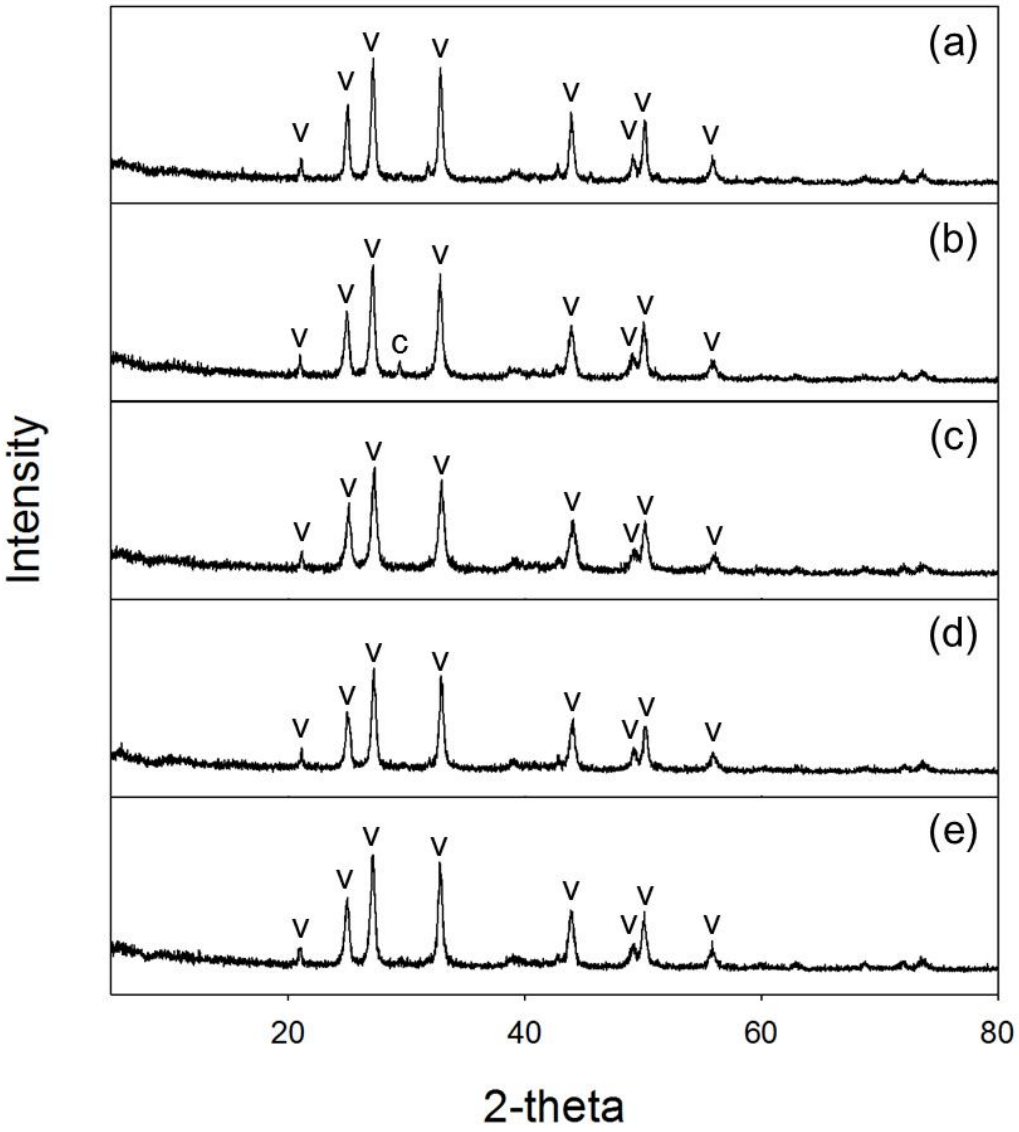

Fig. 16 XRD analysis of the $CaCO_3$ produced using seawater and various raw materials: (a) CKD and seawater, (b) PSA and seawater, (c) CKD and seawater desalination brine, (d) CaO and seawater, (e) $Ca(OH)_2$ and seawater.

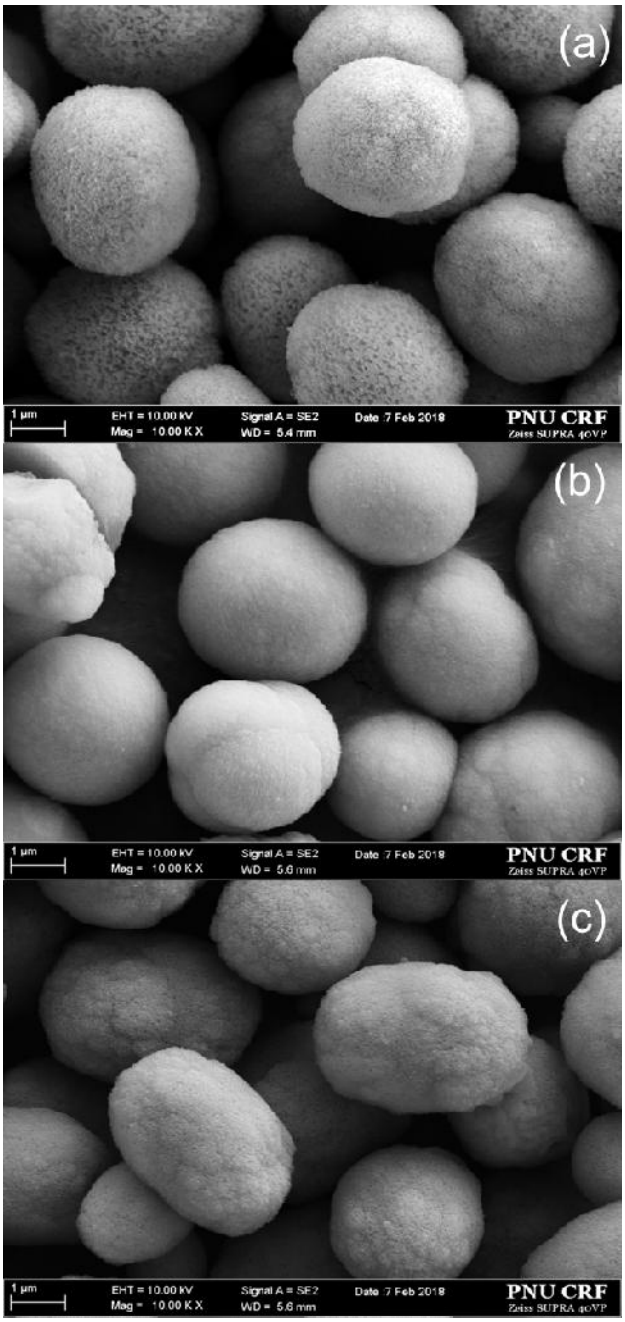

Fig. 17 SEM images of the $CaCO_3$ produced using seawater and various raw materials: (a) CKD and seawater, (b) PSA and seawater, (c) CKD and seawater desalination brine.

3.2.3.3 Influence of carbonation reaction conditions on vaterite formation

The size, shape, and purity of calcium carbonate particles produced under various impeller diameter and stirring speed conditions are compared and summarized in Table 10. The larger the impeller diameter, the greater the content of the vaterite of calcium carbonate produced. For example, when the other conditions are the same and the impeller diameters are different at 70 mm and 50 mm, the content of vaterite of calcium carbonate produced is largely different at 98.2% and 36.1%, respectively. The same conditions except for the impeller diameter were a stirring speed of 300 rpm and a CO_2 flow rate of 3.0 L/min. And when the impeller diameter was small ($Ø_{blade}$: 50 mm), the content of vaterite increased significantly as the stirring speed increased. For example, as the stirring speed increased at 300, 500 and 800 rpm, the vaterite content increased by 36.1%, 72.0% and 97.0%, respectively. The SEM analysis results in Fig. 18 demonstrate that the agitation speed is increased, and nearly 100% vaterite is produced when using a large diameter impeller.The results show that, even though seawater is favored for the formation of vaterite, certain carbonation conditions (impeller diameter, stirring speed) are satisfied in order to produce calcium carbonate with a high content of vaterite .

On the other hand, even if the conditions of the impeller diameter and the stirring speed were changed, the size and purity of the calcium carbonate particles were hardly changed. The particle size of calcium carbonate produced in all experiments was small at 1.96-2.50 μm and the purity was high at 96.50-98.78%.

Table 10 Morphology, particle size and purity of $CaCO_3$ obtained under various carbonation conditions (blade diameter, RPM)

blade diameter (mm)	RPM	CO_2 flow rate (L/min)	$CaCO_3$ morphology		$CaCO_3$ median particle size, D_{50} (μm)	purity (%)
			vaterite (%)	calcite (%)		
50	300	3.0	36.1	63.9	2.23	98.78
	500	3.0	72.0	28.0	1.96	96.56
	800	3.0	97.0	3.0	2.40	98.19
70	300	3.0	100	0	2.29	96.50

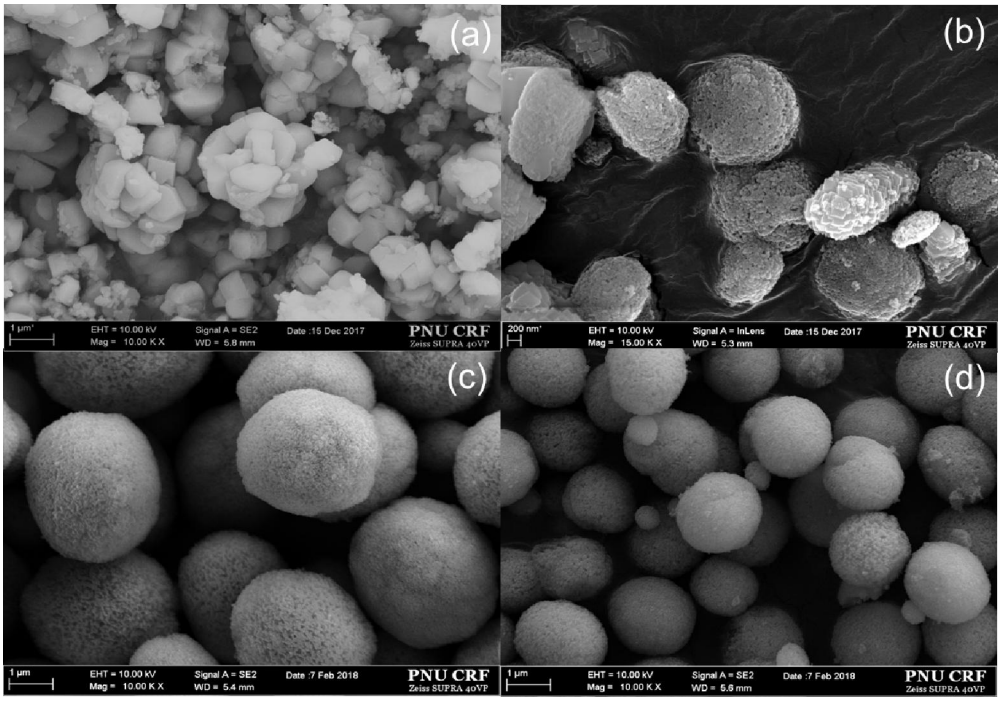

Fig. 18 SEM images of $CaCO_3$ obtained under various carbonation conditions: (a) $Ø_{blade}$: 50mm, 300rpm, (b) $Ø_{blade}$: 50mm, 500rpm, (c) $Ø_{blade}$: 50mm, 800rpm, (d) $Ø_{blade}$: 70mm, 300rpm

3.3 Conclusions

Previous work has used various additives or additional energy to produce the vaterite type calcium carbonate. However, in this study, experiments were conducted to produce the vaterite-type calcium carbonate in a more economical way, using free or low cost seawater as a solvent in the indirect carbonation reaction. It was possible to produce calcium carbonate with 100% vaterite content using seawater compared to four solvents that have been used in the past, and the particle size is also about 2 μm. When various carbon materials (CKD, PSA, CaO, Ca $(OH)_2$) and seawater were used, calcium carbonate having a high content of aterite of 97% or more was generated regardless of the raw materials when the carbonation reaction proceeded. Spherical vaterite produced when seawater was used as a solvent, but when using seawater desalination brine, elliptical vaterite was produced. However, in order to produce calcium carbonate having a content of 100%, it is necessary to meet specific conditions. During the carbonation reaction, the larger the diameter of the stirring impeller, and the higher the stirring speed, the higher the content of the vaterite-type calcium carbonate. The present results show that vaterite-type calcium carbonate that is high-value is produced using only seawater. It different from the existing process of using additives or additional energy. The economic value of the technology is extremely large, as it can produce vaterite using low-cost or free water by taking advantage of the continuously generated industrial by-products.

Chapter 4. Comprehensive conclusion

In this study, seawater was used as a solvent for the indirect carbonation reaction, and the optimum conditions for elution reaction and carbonation reaction using industrial by-products and seawater were derived. n addition, we clarified that seawater is an advantageous solvent for the formation of vaterite-type calcium carbonate through indirect carbonation reaction using seawater, and established the formation conditions of the vaterite-type calcium carbonate. The conclusion of this study is as follows;

1. The component of seawater which elutes calcium from CKD by calcium elution reaction using CKD and seawater was magnesium. The CaO present in the CKD reacted with the magnesium present in the seawater to precipitate the magnesium into magnesium hydroxide, and its motive force was able to elute more calcium than purified water. Furthermore, calcium was able to be eluted at about 5000 mg/L by adding magnesium to seawater.

2. The factors affecting the carbonation efficiency in the carbonation reaction using seawater were the flow rate of carbon dioxide and the amount of added NaOH. The higher the carbon dioxide flow rate, the more carbonation is promoted, and at the same time, the carbonation efficiency also increases. The carbonation efficiency increased as the NaOH dosage increased, indicating 100% carbonation efficiency. As a result of monitoring the pH and calcium concentration during the carbonation reaction, the lowest calcium concentration was shown at pH 10, and the pH optimum for termination of carbonation reaction was determined to 10.

3. It was possible to produce 99.4% pure calcium carbonate through indirect carbonation reaction using seawater. Also, when seawater was used in the indirect carbonation reaction, 184.5 kg-CO_2/ton-waste of carbon dioxide could be

stored and 419.3 kg-$CaCO_3$/ton-waste of calcium carbonate could be produced. By using magnesium-added seawater, the amount of calcium carbonate produced increased to about 615 kg-$CaCO_3$/ton-waste.

4. When comparing seawater with four solvents used as solvents for the existing indirect carbonation reaction, it has been confirmed that seawater is a highly advantageous solvent for the formation of vaterite-type calcium carbonate. And, regardless of the raw material of the indirect carbonation, when seawater was used, it was possible to produce all high content of vaterite type calcium carbonate. In order to produce Vaterite-type calcium carbonate, certain carbonation conditions should be satisfied. During the carbonation reaction, the larger the diameter of the stirring impeller, and the faster the stirring speed, the closer to 100% of the content of vaterite.

Reference

Altiner, M., & Yildirim, M., 2017. Production and characterization of synthetic aragonite prepared from dolomite by eco-friendly leaching–carbonation process. *Advanced Powder Technology*, 28(2), pp.553–564.

Azdarpour, A., Asadullah, M., Mohammadian, E., Hamidi, H., Junin, R., & Karaei, M.A., 2015. A review on carbon dioxide mineral carbonation through pH-swing process. *Chemical Engineering Journal*, 279, pp.615-630.

Azdarpour, A., Asadullah, M., Mohammadian, E., Junin, R., Hamidi, H., Manan, M., & Daud, A.R.M., 2015. Mineral carbonation of red gypsum via pH-swing process: Effect of CO_2 pressure on the efficiency and products characteristics. *Chemical Engineering Journal*, 264, pp.425-436.

Bert Metz, O.D. et al., 2005. *IPCC special report on carbon dioxide capture and storage*. Cambridge University Press:UK.

Bobicki, E.R., Liu, Q., Xu, Z., & Zeng, H., 2012. Carbon capture and storage using alkaline industrial wastes. *Progress in Energy and Combustion Science*, 38, pp.302-320.

Bouquet, E., Leyssens, G., Schönnenbeck, C., & Gilot, P., 2009. The decrease of carbonation efficiency of CaO along calcination–carbonation cycles: Experiments and modelling. *Chemical Engineering Science*, 64(9), pp.2136-2146.

Brečević, L., Nöthig-Laslo, V., Kralj, D., & Popović, S., 1996. Effect of divalent cations on the formation and structure of calcium carbonate polymorphs. *Journal of the Chemical Society, Faraday Transactions*, 92(6), pp.1017–1022.

Chang, R., Kim, S., Lee, S., Choi, S., Kim, M., & Park, Y., 2017. Calcium carbonate precipitation for CO_2 storage and utilization: A Review of the Carbonate Crystallization and Polymorphism. *Frontiers in Energy Research*, 5, pp.17.

Chen, P., Wang, J., Wang, L., Xu, Y., Qian, X., & Ma, H., 2017. Producing

vaterite by CO_2 sequestration in the waste solution of chemical treatment of recycled concrete aggregates. *Journal of Cleaner Production*, 149, pp.735-742.

Cho, T., & Kim, M.J., 2018. Synthesis of magnesium sulfate from seawater using alkaline industrial wastes, sulfuric acid, and organic solvents. *Separation Science and Technology*, pp.1-9.

El Jazairi, B., 1977. The semi-isothermal thermogravimetric technique and the determination of the degree of conversion of high alumina cement concrete. *Thermochimica Acta*, 21(3), pp. 381-389.

Eloneva, S., Teir, S., Salminen, J., Fogelholm, C., & Zevenhoven, R., 2008. Fixation of CO_2 by carbonating calcium derived from blast furnace slag. *Energy*, 9, pp.1461-1467.

Eloneva, S., Teir, S., Salminen, J., Fogelholm, C.J., & Zevenhoven, R., 2008. Fixation of CO_2 by carbonating calcium derived from blast furnace slag. *Energy*, 33(9), pp.1461-1467.

Farhang, F., Oliver, T.K., Rayson, M., Brent, G., Stockenhuber, M., & Kennedy, E., 2016. Experimental study on the precipitation of magnesite from thermally activated serpentine for CO_2 sequestration. *Chemical Engineering Journal*, 303, pp.439-449.

Flaten, E. M., Seiersten, M., & Andreassen, J.P., 2010. Growth of the calcium carbonate polymorph vaterite in mixtures of water and ethylene glycol at conditions of gas processing. *Journal of Crystal Growth*, 312(7), pp.953-960.

Gebauer, D., Völkel, A., & Cölfen, H., 2008. Stable Prenucleation Calcium Carbonate Clusters. *Science*, 322(5909), pp.1819-1822.

Gunning, P.J., Hills, C.D., & Carey, P.J., 2010. Accelerated carbonation treatment of industrial wastes. *Waste management*, 30, pp.1081-1090.

Han, S.J., Im, H.J., & Wee, J.H., 2015. Leaching and indirect mineral carbonation

performance of coal fly ash-water solution system. Applied *Energy*, 142, pp.274-282.

He, L., Yu, D., Lv, W., Wu, J., & Xu, M., 2013. A Novel method for CO_2 sequestration via indirect carbonation of coal fly ash. *Industrial & Engineering Chemistry Research*, 52(43), pp.15138-15145.

Huntzinger, D.N., Gierke, J.S., Kawatra, S.K., Eisele, T.C., & Sutter, L.L., 2009. Carbon dioxide sequestration in cement kiln dust through mineral carbonation. *Environmental Science & Technology*, 43(6), pp.1986−1992.

Jo, H., Jang, Y.N., & Young, J.H., 2012. Influence of NaCl on mineral carbonation of CO_2 using cement material in aqueous solutions. *Chemical Engineering Science*, 80, pp.232−241.

Jo, H., Park, S.H., Jang, Y.N., Chae, S.C., Lee, P.K., & Jo, H.Y., 2014. Metal extraction and indirect mineral carbonation of waste cement material using ammonium salt solutions. *Chemical Engineering Journal*, 254, pp.313-323.

Jo, H.Y., Kim, J.H., Lee, Y.J., Lee, M., & Choh, S.J., 2012. Evaluation of factors affecting mineral carbonation of CO_2 using coal fly ash in aqueous solutions under ambient conditions. *Chemical Engineering Journal*, 183, pp.77-87.

Kester, D.R., Duedall, I.W., Connors, D.N., & Pytkowicz, R.M., 1967. Preparation of artificial seawater. *Limnology and Oceanography*, 12, pp.176-179.

Kezuka, Y., Kawai, K., Eguchi, K., & Tajika, M., 2017. Fabrication of single-crystalline calcite needle-like particles using the aragonite−calcite phase transition. *Minerals*, 7(8), pp.113

Kim, M.J., & Kim, D., 2018. Maximization of CO_2 storage for various solvent types in indirect carbonation using paper sludge ash. *Environmental Science and Pollution Research*, 25(30), pp.30101-30109.

Kim, M.J., Pak, S.Y., Kim, D., & Jung, S., 2017. Optimum conditions for

extracting Ca from CKD to store CO_2 through indirect mineral carbonation. *KSCE Journal of Civil Engineering*, 21(3), pp.629-635.

Krevor, S.C., & Lackner, K.S., 2009. Enhancing process kinetics for mineral carbon sequestration. *Energy Procedia*, 1(1), pp.4867-4871.

Kunzler, C., Alves, N., Pereira, E., Nienczewski, J., Ligabue, R., Einloft, S., & Dullius, J., 2011. CO_2 storage with indirect carbonation using industrial waste. *Energy Procedia*, 4, pp.1010-1017.

Lackner, K.S., Wendt, C.H., Butt, D.P., Joyce, E.L., & Sharp, D.H., 1995. Carbon dioxide disposal in carbonate minerals. *Energy*, 20, pp.1153-1170.

Leggett, C.J., & Rao, L., 2015. Complexation of calcium and magnesium with glutarimidedioxime: Implications for the extraction of uranium from seawater. *Polyhedron*, 95, pp.54-59.

Li, Y., Ma, X., Wang, W., Chi, C., Shi, J., & Duan, L., 2017. Enhanced CO_2 capture capacity of limestone by discontinuous addition of hydrogen chloride in carbonation at calcium looping conditions. *Chemical Engineering Journal*, 316, pp.438-448.

Markewitz, P., Kuckshinrichs, W., Leitner, W., Linssen, J., Zapp, P., Bongartz, R., Schreiber, A., & Müller, T.E., 2012. Worldwide innovations in the development of carbon capture technologies and the utilization of CO_2. *Energy & Environmental Science*, 5, pp.7281-7305.

Morse, J.W., & He, S., 1993. Influences of T, S and P_{CO2} on the pseudo-homogeneous precipitation of CaCO3 from seawater: implications for whiting formation. *Marine Chemistry*, 41(4), pp.291-297.

Mun, M., Cho, H., Kwon, J., Kim, K., & Kim, R., 2017. Investigation of the CO_2 sequestration by indirect aqueous carbonation of waste cement. *American Journal of Climate Change*, 6, pp.132-150.

Na, H.R., & Kim, M.J., 2019. Determination of optimal conditions for magnesium recovery process from seawater desalination brine using paper sludge ash, sulfuric acid, and ethanol. *Desalination Water Treatment*, pp.1-8.

Oral, Ç.M., & Ercan, B., 2018. Influence of pH on morphology, size and polymorph of room temperature synthesized calcium carbonate particles. *Powder Technology*.

Perez-Moreno, S.M., Gazquez, M.J., & Bolivar, J.P., 2015. CO_2 sequestration by indirect carbonation of artificial gypsum generated in the manufacture of titanium dioxide pigments. *Chemical Engineering Journal*, 15, pp.737-746.

Polettini, A., Pomi, R., & Stramazzo, A., 2016. Carbon sequestration through accelerated carbonation of BOF slag: Influence of particle size characteristics. *Chemical Engineering Journal*, 298, pp.26-35.

Price, G.J., Mahon, M.F., Shannon, J., & Cooper, C., 2011. Composition of Calcium Carbonate Polymorphs Precipitated Using Ultrasound. *Crystal Growth & Design*, 11(1), pp.39−44.

Prigiobbe, V., Hänchen, M., Werner, M., Baciocchi, R., & Mazzotti, M., 2009. Mineral carbonation process for CO_2 sequestration. *Energy Procedia*, 1, pp.4885-4890.

Prigiobbe, V., Polettini, A., & Baciocchi, R., 2009. Gas−solid carbonation kinetics of Air Pollution Control residues for CO_2 storage. *Chemical Engineering Journal*, 148, pp.270-278.

Radha, A.V., Forbes, T.Z., Killian, C.E., Gilbert, P.U.P.A., & Navrotsky, A., 2010. Transformation and crystallization energetics of synthetic and biogenic amorphous calcium carbonate. *Proceedings of the National Academy of Sciences of the United States of America*, 107, pp.16438-16443.

Rahmani, O., 2018. CO_2 sequestration by indirect mineral carbonation of industrial

waste red gypsum. *Journal of CO2 Utilization*, 27, pp.374-380.

Rao, M.S., 1973. Kinetics and mechanism of the transformation of vaterite to calcite. *Bulletin of the Chemical Society of Japan*, 46(5), pp.1414-1417.

Rodriguez-Blanco, J.D., Shaw, S., & Benning, L.G., 2011. The kinetics and mechanisms of amorphous calcium carbonate (ACC) crystallization to calcite, via vaterite. *Nanoscale*, 3, pp.265−271.

Sanna, A., Uibu, M., Caramanna, G., Kuusik, R., & Maroto-Valer, M.M., 2014. A review of mineral carbonation technologies to sequester CO_2. *Chemical Society reviews*, 43, pp.8049-8080.

Santos, R.M., Bodor, M., Dragomir, P.N., Vraciu, A.G., Vlad, M., & Gerven, T.V., 2014. Magnesium chloride as a leaching and aragonite-promoting self-regenerative additive for the mineral carbonation of calcium-rich materials. *Minerals Engineering*, 59, pp.71−81.

Shaffer, G., 2010. Long-term effectiveness and consequences of carbon dioxide sequestration, *Nature Geoscience*, 3, pp.464-467.

Sun, Y., Yao, M.S., Zhang, J.P., & Yang, G., 2011. Indirect CO_2 mineral sequestration by steelmaking slag with NH_4Cl as leaching solution. *Chemical Engineering Journal*, 173(2), pp.437-445.

Teir, S., Eloneva, S., Fogelholm, C.J., & Zevenhoven, R., 2009. Fixation of carbon dioxide by producing hydromagnesite from serpentinite. *Applied Energy*, 86, pp.214-218.

Teir, S., Kuusik, R., Fogelholm, C.J., & Zevenhoven, R., 2007. Production of magnesium carbonates from serpentinite for long-term storage of CO_2. *International Journal of Mineral Processing*, 85(1-3), pp.1−15.

Trushina, D.B., Bukreeva, T.V., & Antipina, M.N., 2016. Size-controlled synthesis of vaterite calcium carbonate by the mixing method: aiming for nanosized particles.

Crystal growth & design, 16, pp.1311−1319.

Villain, G., Thiery, M., & Platret, G., 2007. Measurement methods of carbonation profiles in concrete: Thermogravimetry, chemical analysis and gammadensimetry. *Cement and Concrete Research*, 37(8), pp.1182−1192.

Wang, X., & Maroto-Valer, M.M., 2013. Optimization of carbon dioxide capture and storage with mineralisation using recyclable ammonium salts. *Energy*, 51, pp.431−438.

Zhao, H., Park, Y., Lee, D.H., & Park, A.A., 2013. Tuning the dissolution kinetics of wollastonite via chelating agents for CO_2 sequestration with integrated synthesis of precipitated calcium carbonates. *Physical Chemistry Chemical Physics*, 36, pp.15185-15192.

Acknowledgements

저에게 연구할 수 있는 기회를 주시고 2년 동안 많은 것을 공부할 수 있도록 지도해주신 김명진 교수님께 먼저 감사의 인사를 드립니다. 많이 모자랐던 저를 믿고 많은 것을 맡겨주시고, 지도해주셨기 때문에 제가 이 논문을 제출할 수 있었습니다. 연구를 하면서 원하는 방향으로 진행되지 않을 때도 많았고, 실험이 잘 진행되지 않았던 때도 많았습니다. 그때마다 항상 교수님께서는 저에게 격려를 아끼시지 않으셨고, 그 때문에 더 좋은 연구결과가 나왔다고 생각합니다. 언제나 교수님을 생각하며 교수님이 주셨던 가르침 잊지 않도록 하겠습니다.

그리고 좋은 논문이 나올 수 있도록 지도해주신 유경근 교수님과 박영규 교수님께도 감사의 인사를 드립니다. 연구를 진행함에 있어서 미처 생각하지도 못했던 부분에 대해서 다방면의 시각에서 많은 조언을 해 주셨기 때문에, 더 많은 것을 배울 수 있었습니다.

석사과정 중 늘 조언과 관심을 주셨던 성수형, 태연이형께도 감사하다는 말 전하고 싶습니다. 저에게는 두 분이 최고의 사수라고 말씀드리고 싶습니다. 그리고 같이 연구실 생활을 했던 근영이와 선미에게도 고맙다는 말 전하고 싶습니다.

같이 대학원 생활에서 큰 버팀목이 되어주었던 혜림이에게도 이 기쁨을 나누고 싶습니다. 서로 연구에 대해 이야기할 때는 자주 다투기도 했지만, 2년의 시간동안 혜림이가 없었다면 정말 외로운 시간이 되었을 것이라고 생각합니다.

그리고 태선이형, 경근이형, 성관이형, 태남이형, Aalfin, 윤정이, 희소 먼저 졸업한 완철이 모두에게 감사하다는 말씀 전하고 싶습니다.

마지막으로 현재의 제가 있기까지 저의 선택을 존중해주시고, 좋은 말씀 마다하지 않으셨던 우리 부모님과 누나에게 이 큰 기쁨을 드리고 싶습니다.